Pak. J. Bot., 59(4): April 2027.

ARTICLE | DOI: http://dx.doi.org/10.30848/PJB2027-4(13)

THREE-DIMENSIONAL SEED MORPHOLOGY AND EVOLUTIONARY DIVERSIFICATION IN THE GRAPE FAMILY (VITACEAE)

SHAKIR ULLAH[1,2,3], KYAW NYEIN[1,2,3], ZHI-YONG TANG[1,2,3], SHAHAB ALI[1,2,3], MUSHTAQ AHMAD[4,5], LI-MIN LU[1,2,6], CHEN-CHEN ZHENG[1,2,3], LI-NA ZHAO[1,2], ROMER NARINDRA RABARIJAONA[1,2], BING LIU[1,2,6*] AND ZHI-DUAN CHEN[1,2,6]

[1]State Key Laboratory of Plant Diversity and Specialty Crops & Key Laboratory of Systematic and Evolutionary Botany, Institute of Botany, Chinese Academy of Sciences, Beijing 100093, China
[2]China National Botanical Garden, Beijing, China
[3]University of Chinese Academy of Sciences, Beijing 100049, China
[4]Sino-Pak Biodiversity and Bioenergy Research Centre, Department of Plant Sciences, Quaid-i-Azam University, Islamabad, Pakistan
[5]Tashkent State Agrarian University, Department of Medicinal Plants, 2A Universitet Str., Kibray District, 100700, Tashkent region, Uzbekistan
[6]Sino-Africa Joint Research Center, Chinese Academy of Sciences, Wuhan 430074, China

*Corresponding author's email: liubing@ibcas.ac.cn, zhiduan@ibcas.ac.cn

Abstract

The Vitaceae, commonly known as the grape family, is an ecologically and evolutionarily important family of angiosperms distributed across tropical, subtropical, and temperate regions. It comprises five tribes and exhibits marked diversity in seed morphology, yet comprehensive 3D investigations of both internal and external seed structures remain limited. This study aims to document micro-CT-based seed morphometrics and 3D seed morphology in Vitaceae to evaluate variation in chalaza architecture, ventral infolds, endosperm, and seed coat anatomy and to explore their systematic and evolutionary significance. Fourteen species belonging to 12 genera representing all five tribes of Vitaceae were examined, with *Leea* included for comparison. Seeds were analyzed using micro-CT and scanning electron microscopy. A comprehensive set of seed morphological and anatomical characters was documented, including seed size and shape, chalaza length and width, ventral infold dimensions, endosperm configuration, endotesta thickness, and seed coat cellular features. PCA, correlation analysis, ancestral state reconstruction, and phylogenetic signal testing were used to evaluate character variation and evolutionary patterns. Seed morphometric and anatomical analyses revealed substantial interspecific variation in seed size, chalaza morphology, ventral infold architecture, endosperm structure, endotestal thickness, and seed coat anatomy. Seed shapes, chalaza-related traits, ventral infold configuration, and endosperm shape were especially informative for distinguishing species and major lineages. Principal component analyses showed differentiation among species, with internal anatomical traits, particularly endospermic and endotestal characters, providing strong discriminatory signals. Ancestral state reconstructions indicated that several external characters, such as seed shape and surface rumination, evolved repeatedly and exhibited greater homoplasy; in contrast, internal structural traits, especially parts of seed coat anatomy, endotesta, and endosperm, showed stronger phylogenetic structuring. Micro-CT-based analyses demonstrate that Vitaceae seeds are highly diverse in both external form and internal anatomy. Internal structural characters, particularly endotesta architecture, endosperm configuration, and seed coat anatomy, are more evolutionarily stable and taxonomically informative than many external traits. These findings highlight the value of micro-CT as a non-destructive framework for comparative morphology, systematic delimitation, and evolutionary interpretation in Vitaceae.

Key words: Vitaceae; Seed morphology; Micro-CT; Seed anatomy; Ancestral state reconstruction; Phylogenetic signal; Seed evolution.

Introduction

The grape family Vitaceae represents an ecologically and economically significant lineage of flowering plants, distributed across tropical, subtropical, and temperate regions worldwide (Lombardi, 2007, 2015; Lubna *et al.,* 2021). The family comprises approximately 18 genera and nearly 950 species (Wen, 2007; Lu *et al.,* 2018a, 2018b; Anon., 2025). Among them, the genus *Vitis* L. includes the cultivated grapevine, one of the most economically important fruit crops globally (Soejima & Wen, 2006). Beyond viticulture, numerous wild members of Vitaceae play important ecological roles as canopy climbers in forest ecosystems and are utilized locally as edible fruits, medicinal plants, and sources of natural fibers (Wen *et al.,* 2013; Budha-Magar *et al.,* 2020).

Morphologically, Vitaceae are predominantly woody climbers characterized by leaf-opposed tendrils (Süssenguth, 1953). This key structural innovation facilitates climbing and contributes to their ecological success as lianas across diverse vegetation types (Gerrath *et al.,* 2017). In addition to vegetative features, reproductive morphology provides important diagnostic characters (Rabarijaona *et al.,* 2025). Vitaceae seeds are particularly distinctive among angiosperms in possessing a pair of ventral infolds and a prominent dorsal chalazal knot (Chen & Manchester, 2011; Manchester *et al.,* 2013). These characters represent key synapomorphies of the family and have long been used in taxonomic identification (Tiffney & Barghoorn, 1976; Chen & Manchester, 2007). The combination of vegetative and seed features makes Vitaceae morphologically recognizable among rosids (Wilson *et al.,* 2006; Timmons *et al.,* 2007). Vitaceae, together with

Received: 16-07-2026 | Revised: 10-09-2026 | Accepted: 16-09-2026 | Online: 05-11-2026

Leeaceae (genus *Leea*), constitute the order Vitales, which has been inferred to occupy a basal position within the rosid clade based on molecular phylogenetic evidence (Xiao *et al.,* 2021; You *et al.,* 2024). Over the past two decades, molecular systematics has substantially improved our understanding of relationships within the family (Soltis *et al.,* 2000; Rossetto *et al.,* 2007; Nie *et al.,* 2010, 2012). Comprehensive phylogenetic analyses have clarified generic boundaries and recognized five major tribes: Ampelopsideae, Cisseae, Cayratieae, Parthenocisseae, and Viteae (Lu *et al.,* 2012; Wen *et al.,* 2018; You *et al.,* 2024). These phylogenetic frameworks provide a robust basis for investigating character evolution within the family (Lu *et al.,* 2013, 2018; Xiao *et al.,* 2021). However, while molecular relationships are increasingly well resolved, the evolutionary patterns of many morphological characters, particularly those associated with seeds, remain insufficiently explored (Liu *et al.,* 2013, 2016; Manchester, 2020; Lubna *et al.,* 2021).

Seed morphology has long been regarded as taxonomically informative in Vitaceae (Cho *et al.,* 2016; Dang *et al.,* 2016; Adams *et al.,* 2016). Compared with floral characters, which are often fragile and subject to distortion during preservation, seeds are relatively stable structures that retain diagnostic features even in dried herbarium material and fossilized form (Tiffney & Barghoorn, 1976; Gerrath & Posluszny, 1989). The seed develops within the protective environment of the fruit, and many structural characters remain conserved across developmental stages (Godfray & Knapp, 2004; Latiff, 2012). Key seed features in Vitaceae include chalaza shape and position, the depth and configuration of ventral infolds, the development of the raphe ridge, and the organization of seed coat tissues (Latiff, 1982; Habib *et al.,* 2018). In general, seeds of *Cissus*, *Cyphostemma*, *Tetrastigma*, *Rhoicissus*, *Cayratia*, *Causonis,* and *Pseudocayratia* have a long or linear chalaza, like those of *Leea*, whereas seeds of *Ampelopsis*, *Nekemias*, *Clematicissus*, *Ampelocissus*, and *Vitis* possess an oval chalaza (Karkamkar *et al.,* 2010; Habib *et al.,* 2017). Variation in seed coat cellular structure, particularly the presence of columnar versus isodiametric cells, has been shown to differentiate major lineages within Vitaceae and often corresponds to differences in chalaza morphology, such as short versus elongate linear forms (Chen & Manchester, 2007; Manchester *et al.,* 2012). Seed characters have proven especially informative at the generic and infrageneric levels, assisting in the delimitation of closely related genera (e.g., *Parthenocissus* and *Yua*) and in resolving species complexes within larger genera such as *Tetrastigma* (Chen & Manchester, 2011; Habib *et al.,* 2017; Ma *et al.,* 2021). These findings highlight the systematic importance of seed morphological and anatomical traits within the family (Latiff, 1982, 1983; Habib *et al.,* 2018). The family also possesses a rich fossil record, particularly of seeds, which provides crucial evidence for understanding its evolutionary history and historical biogeography (Dorofeev, 1957; Chandler, 1961; Chen, 2009; Rozefelds & Pace, 2018). Fossil seeds of Vitaceae have commonly been identified to extant genera through comparisons of key morphological features, particularly the shape and placement of the chalaza and the morphology of the ventral infolds (Popova & Yakovleva, 2009). Such fossils have contributed to reconstructions of paleogeographic distributions and temporal diversification patterns (Kowalski *et al.,* 2010; Manchester, 1994, 2020). However, accurate fossil placement depends on a comprehensive understanding of morphological variation among living taxa (Moreau *et al.,* 2014). Incomplete sampling of extant seed diversity may therefore limit interpretations of fossil affinities and evolutionary trends (Lu *et al.,* 2016; Dang *et al.,* 2017).

Despite the recognized importance of seed characters, previous studies of seed morphology and seed coat anatomy in Vitaceae have been limited in scope (Najmaddin *et al.,* 2013; Habib *et al.,* 2017, 2018; Parmar *et al.,* 2021). Many investigations have relied primarily on light microscopy and have focused on selected genera or regional floras (Periasamy, 1962; Rabarijaona *et al.,* 2020, 2021). Although scanning electron microscopy (SEM) has been applied in some cases to examine seed surface features, broad comparative analyses across the family remain scarce (Sun *et al.,* 2018; Adams *et al.,* 2016). In particular, detailed assessments of seed coat micromorphology and anatomical variation across multiple tribes are lacking (Schmid, 1986; Tcherepova & Pigg, 2005; Jackes, 2023). Consequently, patterns of seed character diversification and their evolutionary implications within a phylogenetic framework remain incompletely understood (Wen *et al.,* 2014; Trias-Blasi *et al.,* 2021). Advances in microscopic imaging techniques, particularly SEM and micro-CT, allow high-resolution examination of seed surface ornamentation and micromorphological structures that are not readily visible under light microscopy (Najmaddin *et al.,* 2013; Xiong *et al.,* 2021; Song *et al.,* 2022). When integrated with anatomical observations and phylogenetic information, these data provide a powerful approach for investigating morphological evolution (Myles *et al.,* 2011; Moreau *et al.,* 2014). A comprehensive, family-wide study incorporating extensive taxon sampling is therefore necessary to clarify the diversity, structural patterns, and evolutionary significance of seed characters in Vitaceae (Cazaux, 2005; Cervantes *et al.,* 2021). Previous studies of seed morphology, including endosperm shape and seed coat structure, have relied primarily on light microscopy (Chen & Manchester, 2007; Manchester *et al.,* 2013). However, light microscopy provides limited resolution and often requires extensive specimen preparation. In contrast, micro-CT and SEM enable detailed visualization of both internal and external seed structures that are not readily accessible using conventional methods (Heywood, 1969). To date, the application of SEM and micro-CT to investigate internal seed coat anatomy and external seed morphology in extant Vitaceae remains limited.

In the present study, we used broad taxon sampling and advanced imaging techniques to investigate seed morphological diversity and evolutionary trends in the grape family. We systematically examined three-dimensional seed morphology and seed coat anatomy of 14 species representing 12 genera from all five tribes of Vitaceae, as well as the closely related family Leeaceae. The objectives of this study were to: (1) reconstruct and quantify 3D seed morphology in Vitaceae and Leeaceae using micro-CT, providing a comparative framework for evaluating morphological variation across representative genera and tribes; and (2) integrate molecular phylogenetic relationships with ancestral state reconstruction and phylogenetic signal analyses to assess patterns of character evolution and identify major evolutionary trends in seed morphology within Vitaceae.

Materials and Methods

Seed collection and preparation: Seeds were obtained from field collections and herbarium specimens representing major Vitaceae lineages. Samples were preserved in sealed storage boxes. Fourteen species representing 12 genera were selected for micro-CT analysis. The methodological workflow is shown in Figs. S1 and S2, with terminology following Chen (2009) and Chen & Manchester (2007, 2011). For each species, 5 mature seeds were selected for both micro-CT scanning and SEM observation to ensure consistent representation of seed morphological and anatomical variation. Voucher information and specimen details are provided in Table S1.

Sample preparation, mounting, and image acquisition: Micro-CT requires minimal sample preparation compared with conventional anatomical techniques (Diels *et al.,* 2017). Seeds were dehydrated to minimize imaging artifacts, mounted vertically on glass rods using double-sided wax, and supported with low-density materials to reduce X-ray interference during scanning (Moreau *et al.,* 2014). High-resolution X-ray images of Vitaceae seeds were acquired using a SkyScan 1172 micro-CT scanner (Bruker, Billerica, USA). The system was equipped with a microfocus X-ray source (20–100 kV) and an 11-megapixel detector with a 12-bit cooled CCD camera.

Each seed specimen was scanned from the base to the apex using 1000–1150 projections during a 360° rotation, with an acquisition time of approximately 3 h 35 min per seed, allowing complete visualization of both external and internal seed structures. The specimens ranged from 8.72 to 9.47 mm in length and were scanned at approximately 1133 projections mm^{-1} to obtain high-resolution 3D reconstructions. Scanning was performed at 40 kV and 250 μA to optimize structural preservation and image quality. Raw projection images were saved in TIFF format and reconstructed using NRecon (v1.6.9.3, Bruker) into cross-sectional image stacks (1000 × 1000 pixels) in BMP format. Detailed scanning parameters, including pixel size, exposure conditions, and acquisition settings, are provided in Table 1 (Diels *et al.,* 2017).

Table 1. Scanning parameters for CT imaging.

Parameters	Values
Scanner	Skyscan 1172
Camera	Hamamatsu C9300
Camera pixel size	8.82 μm
Image pixel size	11.77 μm
Depth	16 bits
Exposure time	3 hr 35 min
Source voltage	40 kV
Source current	250 μA
Camera binning	4x4
Object-to-source distance	70.310 mm
Camera-to-source distance	210.666 mm

Micro-CT image preprocessing and reslicing: Image preprocessing and analysis were conducted in MATLAB (v2015a) (Cazaux *et al.,* 2005). Pattern-recognition procedures were performed using the Balu toolbox (http://dmery.ing.puc.cl/index.php/balu) and VLFeat (v0.9.20; http://www.vlfeat.org/index.html) for image feature extraction, feature selection, and exploratory classification of CT image patterns. These computational approaches provide functions for image transformation, clustering, and performance evaluation (Fernandes *et al.,* 2016). The extracted image features were used to evaluate structural similarities among seed images and were not considered substitutes for biological measurements. Quantitative morphological and anatomical traits used for comparative and evolutionary analyses were obtained independently from 3D reconstructed seed structures. For seeds <10 mm, each specimen comprised 1000–1150 XY-plane slices representing virtual cross-sections from the base to the apex (Fernandes *et al.,* 2016). To improve visualization of internal structures, image stacks were resliced into XZ (sagittal) and YZ (frontal) planes (Figs. S1–S2), generating 30 slices per plane (Adams *et al.,* 2016).

Image quality enhancement: Image enhancement, including intensity and contrast adjustment, is an essential step in micro-CT image processing (Adams *et al.,* 2016). Following Verboven *et al*., (2008), 5 representative images per seed (three XY slices, one XZ slice, and one YZ slice) were selected based on the maximum endosperm area (Cazaux *et al.,* 2005). Three enhanced datasets (Set_A, Set_B, and Set_C) were generated following previous image-processing approaches (Adams *et al.,* 2016). Set_A involved intensity normalization and scaling (Dhondt *et al.,* 2010), whereas Set_B applied mean adjustment, normalization, and top-hat/bottom-hat transformations to improve contrast and reduce noise (Fernandes *et al.,* 2016). Median filtering using a 3 × 3 window was applied to generate Set_C while preserving structural boundaries (Dhondt *et al.,* 2010). In total, 15 processed images per seed (three XY, one XZ, and one YZ images from each enhanced dataset) were used for subsequent segmentation analysis (Fernandes *et al.,* 2016).

Micro-CT image segmentation (binary mask) and feature extraction: Image segmentation divides images into regions based on pixel intensity values, allowing separation of similar and dissimilar areas within the image (Dhondt *et al.,* 2010). In this study, the entire seed was defined as the region of interest (ROI), and segmentation was performed using balanced histogram thresholding to distinguish foreground (seed = 1) from background (air = 0). Threshold values were derived from image histograms following the approach described by Verboven *et al*., (2008).

Feature extraction was performed to characterize image-based structural patterns, including intensity, texture, and local image features, rather than to replace direct biological measurements of seed morphology (Fernandes *et al.,* 2016). Features were extracted from enhanced image datasets (Set_A, Set_B, and Set_C), generating 348 image descriptors per image. By combining 15 processed images per seed, a 5,220-dimensional image feature vector was generated for each sample (Verboven *et al.,* 2008). These extracted features were used for exploratory image classification and structural comparison, whereas quantitative morphological and anatomical traits were measured independently from 3D reconstructed seed structures. The extracted image features are summarized in Table 2. Segmentation quality was evaluated through visual inspection of binary masks and reconstructed seed volumes.

Thresholding results were checked across representative samples to confirm consistent separation between seed structures and surrounding air (Dhondt *et al.,* 2010). When necessary, segmentation boundaries were manually inspected and corrected to ensure accurate representation of seed contours and anatomical structures, thereby minimizing potential bias associated with threshold selection during image processing (Fernandes *et al.,* 2016).

Table 2. Characteristics of image features extracted from each CT image.

Parameter	Feature name	Number of features
Intensity	Basic intensity	6
Local binary patterns	LBP	242
Intensity	Gabor intensity	67
Contrast	Basic contrast	5
Texture	Haralick texture	28

Three-dimensional seed morphology image reconstruction: Two-dimensional X-ray projection images from each micro-CT scan were reconstructed into 3D images using NRecon (v1.7.3; www.bruker-microct.com) with a filtered back-projection algorithm (Verboven *et al.,* 2008). Ring artefact and beam hardening corrections were applied at 10% and 30%, respectively (Moreau *et al.,* 2014). Regions of interest (ROIs) containing individual seeds were then isolated using Data Viewer (v1.5.6.2; www.bruker-microct.com) for analysis of internal and external morphology.

Qualitative and quantitative seed morphology: Visual examination of the internal seed structure was conducted using CTvox software (version 3.3.0; www.bruker-microct.com). The software allowed 3D visualization of internal seed structures. Anatomical features were examined and identified according to the terminology and descriptions provided in previous studies (Chen & Manchester, 2011; Manchester *et al.,* 2013). Quantification of volumetric and morphological traits was conducted on the reconstructed 3D images using an object-based image analysis approach (e.g., Dhondt *et al.,* 2010; Fernandes *et al.,* 2016).

Process of reconstruction software and image visualization: The field of view was cropped to reduce volume and improve computational efficiency. Output files were saved in 16-bit format to preserve detail and dynamic range (Verboven *et al.,* 2008). The rotation axis was determined automatically from central pixels across the projections (Verboven *et al.,* 2008), and beam-hardening correction was applied to reduce reconstruction artifacts (Dhondt *et al.,* 2010). Background normalization was performed to compensate for scattering and brightness variation (Fernandes *et al.,* 2016). Reconstructed data were visualized using both volume and surface rendering approaches (Dhondt *et al.,* 2010).

Scanning electron microscopy observation of the seed coat: Seeds were fixed in FAA (glutaraldehyde), dehydrated through an ethanol series (60% for 3 h, 70% for 3 h, 80% for 3 h, 90% for 3 h, 95% for 3 h, and 100% overnight), mounted on stubs, and gold-coated (Song *et al.,* 2022). Samples were examined using a JSM-IT500 SEM (IBCAS) at 30–50×, 200×, and 800× magnifications (20 kV, 2 mm working distance). Seed coat surface pattern, shape, and epidermal cell structure were described following Chen & Manchester (2011) and Manchester *et al*., (2013).

Data analysis: Micro-CT data were analyzed to visualize the three-dimensional internal seed structure using CTvox software (v3.3.0; Bruker MicroCT) (Verboven *et al.,* 2008; Fernandes *et al.,* 2016).

Character definition, coding, and state delimitation: Morphological and anatomical characters were defined and coded following established seed morphological terminology used in Vitaceae studies (Tiffney & Barghoorn, 1976; Chen & Manchester, 2007; Chen, 2009). The character matrix (Table S2) included both qualitative and quantitative traits derived from micro-CT reconstructions and SEM observations. Qualitative characters, including seed shape, seed surface ornamentation, dorsal chalaza morphology, chalaza groove characteristics, ventral infold configuration, endosperm shape, and seed coat micromorphological features, were coded according to discrete morphological states observed among taxa. These states were defined based on comparative examination of reconstructed seed structures and previously established morphological terminology. Quantitative characters were measured directly from three-dimensional micro-CT reconstructions and converted into ordered character states using predefined thresholds based on observed morphological variation among sampled taxa. For example, seed dimensions, chalaza dimensions, ventral infold dimensions, endosperm dimensions, and anticlinal wall thickness were categorized into discrete states according to their measured ranges (Table S2). The threshold values were selected to represent biologically meaningful differences among taxa rather than arbitrary divisions. All character states were evaluated through repeated examination of micro-CT and SEM datasets to ensure consistency of coding. Micro-CT segmentation and threshold selection were visually inspected during reconstruction, and anatomical boundaries were verified against reconstructed three-dimensional structures to minimize potential measurement bias.

Phylogenetic tree and evolutionary model assumptions: Ancestral state reconstruction was performed for seed characters relevant to Vitaceae classification (Table S3) using the coded character matrix described above. The phylogenetic framework was obtained by extracting the 14-taxa Vitaceae phylogeny from You *et al*., (2024). The sampled taxa represented 12 genera distributed across all five recognized tribes of Vitaceae, with *Leea* included as the outgroup for rooting the phylogenetic tree. The extracted phylogeny was used as the backbone for ancestral state reconstruction and phylogenetic comparative analyses. Trait evolution was evaluated under alternative evolutionary models, including Brownian motion (BM), Ornstein–Uhlenbeck (OU), and Early Burst (EB), using the R packages phytools (Revell, 2012) and geiger. Model performance was compared using corrected Akaike information criteria (AICc), and the most appropriate evolutionary model was selected based on the lowest AICc value (Tables S9–S10).

Phylogenetic signal of morphological and anatomical traits was assessed using Pagel's λ (Pagel, 1999) and Blomberg's K (Blomberg *et al.,* 2003) under a Brownian motion framework. Pagel's λ values approaching 1 indicate strong phylogenetic dependence, whereas values near 0 suggest weak phylogenetic association. Blomberg's K values greater than 1 indicate stronger phylogenetic conservatism than expected under Brownian motion, whereas values below 1 indicate weaker phylogenetic structure (Tables S9–S10).

Correlation analysis, bar plot, and principal components analysis: Pearson correlations among seed traits were computed in R (v4.3.1) and visualized as a clustered heatmap (pheatmap) using pairwise complete observations. Morphological data of the seed were measured in ImageJ and plotted in ggplot2 to show interspecific variation. PCA was performed in R (v4.3.2) to assess multivariate patterns, with results visualized as genus-based scatter plots with 95% confidence ellipses; scores and loadings are provided in Tables S5–S8.

Results

Micro-CT morphometrics and 3D seed morphology of Vitaceae: Seed morphology was examined in 14 species representing 12 genera across all five Vitaceae tribes (Cayratieae, Cisseae, Parthenocisseae, Viteae, and Ampelopsideae), with Leeaceae included for comparison (Figs. 1–2 and Table S4). Fig. 3 and Table S4 show anatomical features. Micro-CT analysis revealed substantial interspecific variation in seed size: length ranged from 3 mm in *Tetrastigma planicaule* to 9 mm in *Cyphostemma currorii*, and width from 2 mm in *Tetrastigma planicaule* to 5.5 mm in *Cayratia geniculata* (Figs. S9A–B; S11A–B). The apex-to-widest-point distance varied from 0.4 mm in *Cissus hastata* to 0.6 mm in *Tetrastigma rumicispermum* (Fig. S11E). Apical notch depth ranged from 0.01 mm in *C. geniculata* to 0.9 mm in *Causonis corniculata* (Fig. S11F). Most species possessed a distinct beak, ranging from 0.04 mm in *C. currorii* to 0.1 mm in *Ampelopsis brevipedunculata* (Fig. S11G).

A prominent chalaza was present in all seeds, with length ranging from 0.2 mm in *Vitis betulifolia* to 0.9 mm in *C. hastata* (Figs. S9C; S11H). Chalaza width varied from 0.1 mm in *C. corniculata* to 0.4 mm in *Nekemias arborea*, and thickness from 0.02 mm in *Ampelocissus elephantina* to 0.09 mm in *C. geniculata* (Figs. S9D; S11I). Chalazal positional relationships also varied: the apex-to-widest-point distance ranged from 0.2 mm in *C. corniculata* to 0.6 mm in *C. hastata* (Fig. S11K), the chalaza–notch distance from 0.1 mm in *C. currorii* and *V. betulifolia* to 0.2 mm in *Yua thomsonii* (Fig. S11L), and the chalaza–beak gap from 0.2 mm in *C. currorii* to 0.4 mm in *C. geniculata* and *Y. thomsonii* (Fig. S11M). All examined seeds possessed a well-developed endosperm, with length ranging from 1.5 mm in *Y. thomsonii* to 3.5 mm in *C. currorii*, and width from 2.5 mm in *V. betulifolia* to 6.5 mm in *T. jinghongense* (Figs. S10C–D; S11A–B). The testa, derived from the outer integument, consists of a sarcotesta and lignified endotesta (Periasamy, 1962; Corner, 1976). Overall endotesta thickness ranged from 0.02 mm in *C. currorii* to 0.05 mm in *V. betulifolia*, with maximum thickness from 0.03 mm in *C. currorii* to 0.07 mm in *C. hastata* (Figs. S11N–O). Thickness at the chalaza (1.3 mm in *T. rumicispermum* to 3.0 mm in *T. planicaule*) exceeded that at ventral infolds (0.01 mm in *C. currorii* to 0.04 mm in *C. corniculata*) (Fig. S12A–B). At the ruga apex, thickness ranged from 1.5 mm in *C. geniculata* to 3.5 mm in *C. hastata*, and at the ruga sinus from 0.2 mm in *C. geniculata* to 0.5 mm in *V. betulifolia* (Figs. S12C–D). A pair of ventral infolds was present in all seeds. Infold length ranged from 0.3 mm in *C. hastata* to 0.8 mm in *A. elephantina*, and width from 0.1 mm in *C. currorii* to 0.4 mm in *C. geniculata* (Figs. S10A–B; S12E–F). The length/width ratio varied from 1 in *C. geniculata* to 8 in *C. corniculata* (Fig. S12G). Spacing between infolds ranged from 0.2 mm in *T. rumicispermum* to 0.8 mm in *Leea sambucina* at the apex, 0.2 mm in *C. currorii* to 0.5 mm in *C. corniculata* at the base, and 0.1 mm in *T. planicaule* to 0.9 mm in *L. sambucina* at the middle (Figs. S12H–J). Infold depth ranged from 0.4 mm in *C. corniculata* to 0.7 mm in *A. brevipedunculata*, and the distance to the beak ranged from 0.1 mm (e.g., *A. elephantina*) to 0.3 mm in *T. rumicispermum* (Figs. S12K–L). Transverse section height ranged from 1.5 mm in *Y. thomsonii* to 4.5 mm in *T. jinghongense*, and width from 3 mm in *V. betulifolia* to 7 mm in *T. jinghongense* (Figs. S12M–N). Anticlinal wall thickness ranged from 6 μm in *N. arborea* to 20 μm in *A. brevipedunculata* and was categorized as thin (<15 μm) and thick (≥15 μm) (Fig. S12O). Among the measured traits, chalaza dimensions, ventral infold configuration, endosperm morphology, and endotesta thickness showed the greatest variation among sampled lineages, suggesting their potential value for distinguishing major taxonomic groups within Vitaceae.

Seed morphology of vitaceae based on 3D micro-CT images: Seed morphological characters were examined across representatives of all five tribes of Vitaceae. This dataset provides a broad overview of seed variation and supports comparative evaluation of morphological, anatomical, and potential evolutionary patterns. 3D micro-CT analysis revealed substantial variation in seed size, shape, chalazal structure, and ventral infolds, as well as in seed coat characteristics (cell number, cell shape, anticlinal and periclinal wall thickness) and endosperm morphology. Seed shapes were predominantly obovoid (Fig. 1B1), triangular (Fig. 1A1), elliptic (Fig. 1D1), pyriform (Fig. 2F1), ellipsoid (Fig. 1F1), and oblong (Fig. 2G1). Dorsal radiate markings varied among species, being deep in *C. corniculata* (Fig. 1A1), shallow in *C. hastata* (Fig. 1G1), and absent in *V. betulifolia* (Fig. 2D1). Raphe ridges were less prominent on the ventral surface, and the seed surface rumination patterns radiated from the center toward the margins. Rumination patterns were categorized as smooth, horizontal, irregular, or muricate (Fig. 1B1; Fig. 1A1; Fig. 2E1). Apical notch morphology was classified as bilobed (Fig. 1A1) or retuse (Fig. 2C1). Most species, such as *C. corniculata* (Fig. 1A1), possess a prominent beak with an acute or acuminate apex, whereas *Nekemias arborea* (Fig. 2B1) shows an inconspicuous beak. Based on development, beaks were categorized as prominent (*C. hastata*, Fig. 1G1) or reduced (*A. elephantina*, Fig. 2C1), and by shape as conical-pointed (*C. corniculata*, Fig. 1A1) or cylindrical (*V. betulifolia*, Fig. 2D1).

Dorsal chalaza in Vitaceae: The chalaza is deeply sunken in most examined species. In obovoid and elliptic seeds, the apical notch is widely spread (>155°) (Figs. 2A1–B1), whereas triangular seeds show a grooved apical margin (Fig. 1A1). An elongated dorsal chalazal knot (L/W ≥ 4) extends to the middle (Figs. 1B1; 2A1) or across the entire dorsal surface (Fig. 1F1), while centrally positioned chalazae are oval to pyriform (L/W < 4) (Fig. 2D1). Chalaza length ranges from 1/2 of seed length in *V. betulifolia* (Fig. 2D1) to 2/3 in *T. jinghongense* (Fig. 1E1). Species with L/W ≥ 4 (e.g., *A. elephantina*, Fig. 2C1) show elongated chalaza, whereas those with L/W < 4 (e.g., *V. betulifolia*, Fig. 2D1) exhibit rounded to pyriform forms. Dorsal chalaza shape varies from linear (*T. rumicispermum*, Fig. 1C1) to oval (*V. betulifolia*, Fig. 2D1) and perichalazal (*C. hastata*, Fig. 1G1). Both apical and basal chalazal grooves occur: the apical groove is broad and deep in *V. betulifolia*, narrow and shallow in *T. rumicispermum*, and absent in *T. jinghongense*; the basal groove is broad and deep in *N. arborea*, narrow and shallow in *Y. thomsonii*, and absent in *P. laetevirens* (Figs. 1C1; 1E1; 2B1; 2D1–F1). Chalaza position varies from apex to middle (*C. currorii*, Fig. 1F1), central (*Parthenocissus laetevirens*, Fig. 2E1), or extending from apex to base (*A. elephantina*, Fig. 2C1).

Ventral infolds: A pair of ventral infolds is present on the ventral seed surface, typically diverging toward the margins at different positions. Divergence begins at the base in *C. currorii* (Fig. 1F 2), from the middle in *T. planicaule* (Fig. 1D 2), or remains parallel from base to apex in *A. elephantina* (Fig. 2C2). Basally diverging infolds generally cover ½–¾ of the seed surface, whereas those diverging from the middle extend along most or all of the seed length, except in *T. planicaule*, where they do not reach full length (Fig.1D2). External margins of the ventral infold are smooth in *C. currorii* (Fig. 1F2) and rough in *C. corniculata* (Fig. 1A2). Infolds typically occupy ½–2/3 of the seed length (e.g., *C. hastata*, Fig. 1G2), but extend the full length in *T. planicaule* (Fig. 1D2). Transverse sections show variation in penetration depth, reaching ~½ of the seed in *C. corniculata* (Fig. 1A2) and nearly 2/3 in *T. jinghongense* (Fig. 1E2). The raphe between infolds was distinct, being aequilate in *T. planicaule* (Fig. 1D2) and tapering in *P. laetevirens* (Fig. 2E2). Ventral holes were present in some species but absent in others. Furrows varied in extent, extending from base to apex in *C. corniculata* (Fig. 1A2), from middle to apex in *C. hastata* (Fig. 1G2), and from base to middle in *T. rumicispermum* (Fig. 1C 2). Ventral-view morphology showed further diversity: infolds were keel-shaped in *C. currorii* (Fig. 1F2), cup-shaped in *C. geniculata* (Fig. 1B2), obelliptic in *V. betulifolia* (Fig. 2D2), furrow-shaped in *A. elephantina* (Fig.2C2), and inconspicuous in *T. rumicispermum* (Fig. 1C2). In transverse section, most species (e.g., *C. corniculata*, Fig. 1A5) exhibited deep, concave infolds, whereas *A. elephantina* (Fig. 2C5) showed shallower, horseshoe-shaped structures.

Endotesta thickness and endosperm shape: The testa of Vitaceae seeds originates from the outer integument and consists of a soft sarcotesta and a lignified endotesta (Periasamy, 1962; Corner, 1976). Endotesta thickness varied markedly among species, being thick in *V. betulifolia* (Fig. 2D5), intermediate in *C. currorii* (Fig. 1F5), and thin in *P. laetevirens* (Fig. 2E5). Regional variation was also evident: at the ruga sinus, thickness was thin in *C. geniculata* (Fig. 1B5), intermediate in *A. brevipedunculata* (Fig. 2A5), and thick in *V. betulifolia* (Fig. 2D5); at the chalaza, it was thick in *C. currorii* (Fig. 1F5), intermediate in *Y. thomsonii* (Fig. 2F5), and thin in *A. elephantina* (Fig. 2C5). The shape of the endosperm in transverse section was highly variable among the examined species. An M-shaped endosperm was present in *T. planicaule* (Fig. 1D5) and *N. arborea* (Fig. 2B5); in contrast, other configurations included U-shaped endosperm in *C. geniculata* (Fig. 1B5) and a Y-shaped endosperm in *L. sambucina* (Fig. 2G5). In *C. corniculata* (Fig. 1A5), the endosperm exhibited distinct angular configuration. In some species, deep rugal constrictions were associated with ventral infolds that penetrated the endosperm, producing irregular shapes ⊤.

Seed coat anatomy of Vitaceae: The seed coat of Vitaceae shows considerable variation in cell number, wall structure, surface morphology, air space, and anticlinal wall thickness. Based on cell number, four types were recognized: one layer in *T. rumicispermum* (Fig. 3I), two in *C. corniculata* (Fig. 3C), three in *V. betulifolia* (Fig. 3M), and four in *L. sambucina* (Fig. 3N). Surface cell morphology varied, with 3–4-sided cells in most species (e.g., *C. geniculata*), 4–5-sided in *L. sambucina*, and 5–6-sided in *P. laetevirens*. Anticlinal walls were either raised (*T. planicaule*, Fig. 3K) or grooved (*C. corniculata*, Fig. 3C), with variation in lignification and thickness. Periclinal walls were generally smooth (e.g., *T. planicaule*, Fig. 3F) but irregular in *A. brevipedunculata* (Fig. 3B). Air space between endosperm and testa was present in *N. arborea* (Fig. 2J) but absent in *C. corniculata* (Fig. 1E). Anticlinal wall thickness also varied, being >10 µm in most species (e.g., *T. jinghongense*, Fig. 3J) and <10 µm in *C. hastata* (Fig. 3E). Among the examined characters, chalaza configuration, ventral infold morphology, endosperm shape, and seed coat anatomical traits showed substantial variation among lineages, indicating their potential utility for taxonomic discrimination within Vitaceae.

Seed character evaluation based on 3D micro-CT images: Seed morphological characters were analyzed across 14 species representing 12 genera and five tribes of Vitaceae, with Leeaceae included for comparison. Mapping of these traits onto the molecular phylogeny revealed evolutionary patterns and correspondence between seed morphology and phylogenetic relationships. Ancestral state reconstruction indicated that many seed characters showed well-resolved ancestral states across the phylogeny. Distinct morphological traits were consistently associated with specific lineages, highlighting their taxonomic and evolutionary significance within Vitaceae.

Seed shape and surface rumination pattern: The ancestral state of seed shape was reconstructed as obovoid under the maximum-likelihood framework. Triangular and ellipsoid shapes were restricted to Cayratieae, while the

elliptic shape evolved independently in Cayratieae and Viteae. The pyriform shape was confined to Parthenocisseae (Fig. 4A). Seed shape showed a relatively high Pagel's λ value, but the phylogenetic signal was not statistically significant based on either Pagel's λ or Blomberg's K (Table S9). Ancestral reconstruction indicated smooth seed surface rumination as the ancestral condition in Vitaceae, with no significant phylogenetic signal detected for seed surface rumination pattern based on Pagel's λ and Blomberg's K (Fig.4B and Table S9).

Dorsal radiate markings' appearance: Dorsal radiate markings showed substantial variation across Vitaceae. Ancestral reconstruction indicated the shallow type as ancestral for Cisseae and Viteae, while Cayratieae exhibited all three states, suggesting multiple independent transitions. In contrast, markings were absent in Parthenocisseae and Ampelopsideae, indicating a complete loss in these lineages (Fig. 6B). No significant phylogenetic signal was detected for dorsal radiate markings appearance based on Pagel's λ and Blomberg's K (Table S9).

Number of seed coat cells and surface cell shape: Four seed coat cell-layer states were recorded. Ancestral reconstruction indicated a 2-celled condition as ancestral in Cayratieae and Ampelopsideae, with independent evolution of the 1-celled state in Cayratieae, Parthenocisseae, and Viteae. The 3-celled condition arose in Cayratieae and Viteae, and a 4-celled state evolved within Cayratieae (Fig. 4C). Seed coat cell number showed significant phylogenetic dependence based on Pagel's λ, although Blomberg's K did not provide significant support (Table S9). Surface cell shapes were grouped into three types, with 3–4-sided cells reconstructed as ancestral in Cayratieae and Viteae. The 5–6-sided type evolved independently in Parthenocisseae and Ampelopsideae (Fig. 4D). Surface cell shape showed significant phylogenetic dependence based on Pagel's λ, whereas Blomberg's K indicated weak phylogenetic structuring (Table S9).

Air space between the endosperm and the seed coat: The air space between the endosperm and the seed coat varied among species. Ancestral reconstruction indicated presence as ancestral in Cayratieae and Ampelopsideae, and absence in Cisseae, with both states occurring in Cayratieae, Parthenocisseae, and Viteae, suggesting multiple transitions (Fig. 5A). Phylogenetic signal was relatively high based on Pagel's λ, although Blomberg's K did not provide significant support (Table S9).

Anticlinal and periclinal wall structure: Anticlinal wall structure varied between raised and grooved types. Ancestral reconstruction identified the raised condition as ancestral in Cayratieae, Cisseae, Viteae, and Ampelopsideae, with the grooved type evolving convergently (twice in Cayratieae and once in Parthenocisseae) (Fig. 5C). Anticlinal wall structure showed significant phylogenetic dependence based on Pagel's λ, although Blomberg's K did not provide significant support (Table S9). Periclinal wall structure varied from smooth to uneven. The uneven type was ancestral in Cayratieae, whereas the smooth type was ancestral in Cisseae and Parthenocisseae. Both states occurred in Viteae and Ampelopsideae, indicating multiple transitions, with independent evolution of the smooth type within Cayratieae (Fig. 5D). Periclinal wall structure showed significant phylogenetic dependence based on Pagel's λ, whereas Blomberg's K indicated no significant phylogenetic signal (Table S9).

Dorsal chalaza and position: Chalaza morphology varied among tribes. In Cayratieae, a linear chalaza (length/width ratio ≥ 4; Fig. S4C) was predominant and reconstructed as ancestral. In Cisseae, the chalaza was perichalazal (length/width ratio ≥ 4). In Parthenocisseae, Viteae, and Ampelopsideae, both linear and oval types (length/width ratio ≤ 4; Fig. S4C) occurred, indicating multiple transitions among lineages (Fig. 6A). Dorsal chalaza morphology showed significant phylogenetic structuring based on both Pagel's λ and Blomberg's K, indicating strong evolutionary conservatism of this trait (Table S9). Chalaza position varied among Vitaceae species. Ancestral reconstruction indicated the apex-to-base position as ancestral in Cisseae. In Cayratieae, Viteae, and Ampelopsideae, both apex-to-base and apex-to-middle positions occurred, suggesting multiple shifts, while Parthenocisseae showed apex-to-base and middle positions, indicating repeated transitions (Fig. 6C). Chalaza position showed no significant phylogenetic signal based on Pagel's λ or Blomberg's K (Table S9).

Ventral infolds size and position: Ventral infolds showed marked variation, with two types: narrow and wide. Ancestral reconstruction indicated the narrow type as ancestral in all tribes except Viteae. In Cayratieae and Viteae, both types occurred, suggesting multiple transitions (Fig. 5B). Ventral infold size showed significant phylogenetic structuring based on both Pagel's λ and Blomberg's K, indicating phylogenetic association of this trait (Table S9). Ventral infold size varied among species, with two states: short and long. Ancestral reconstruction indicated the long state as ancestral for Cayratieae and Parthenocisseae, and the short state for Cisseae and Ampelopsideae, with independent origins of the short state in Cayratieae and Viteae (Fig. 6D). Ventral infold position also showed significant phylogenetic dependence based on Pagel's λ, although Blomberg's K did not provide significant support (Table S9).

Phylogenetic signal of seed morphological traits: Phylogenetic signal analyses revealed variable evolutionary conservatism among seed morphological and anatomical traits (Tables S9–S10). Several characters associated with chalaza and ventral infold morphology showed significant phylogenetic structuring, particularly dorsal chalaza, chalaza length traits, ventral infold size, ventral infold width, and ventral infold-related structural characters. In contrast, several seed surface, seed coat, and general size-related traits showed weak or non-significant phylogenetic signals. These results indicate that different components of seed morphology have experienced different evolutionary constraints across Vitaceae lineages.

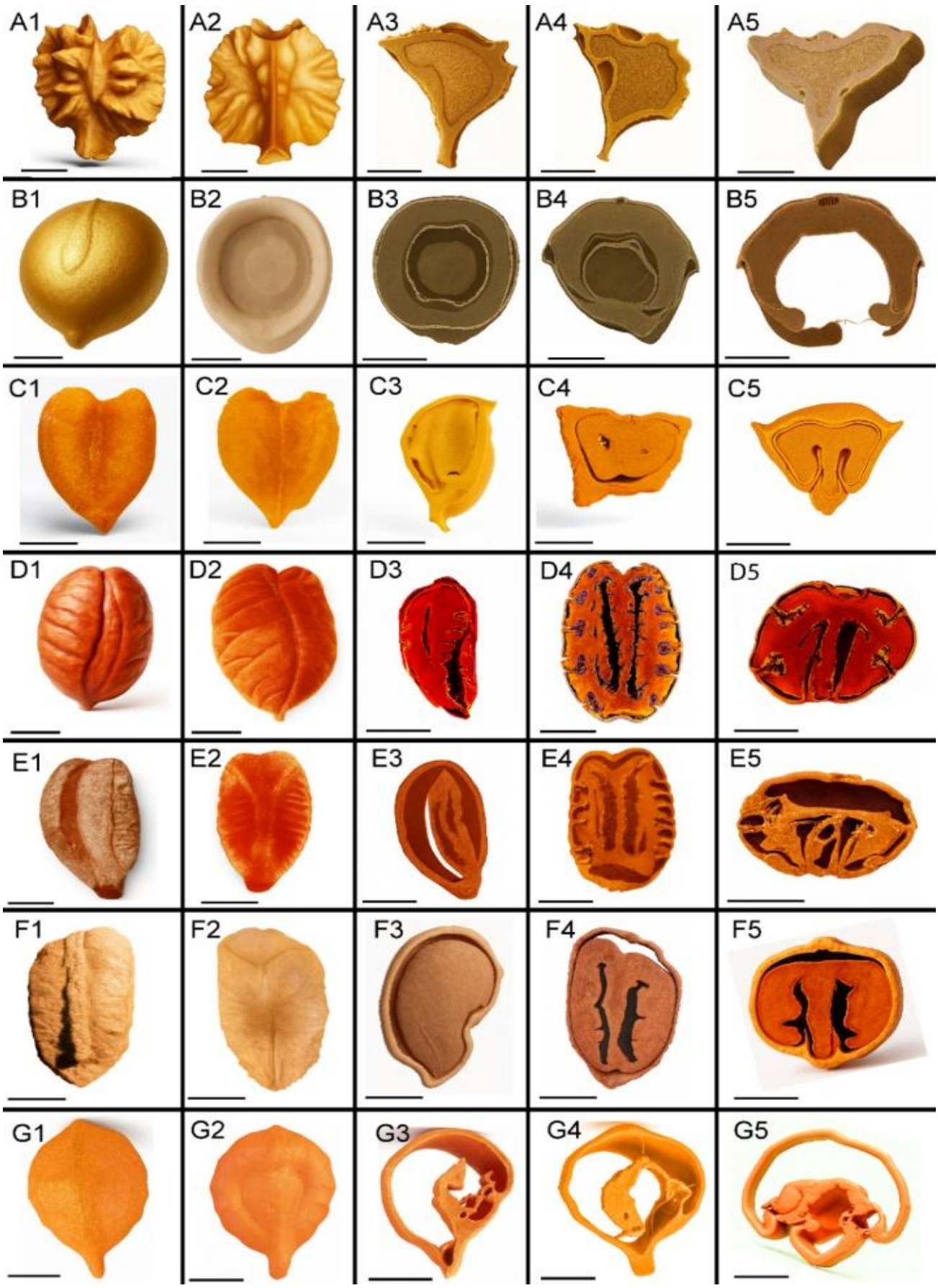


Fig. 1. Micro-CT image used for 3D reconstruction of the seed of the representative species from the family Vitaceae. Dorsal, Ventral, YZ-plane-slice (frontal plane), XZ-plane-slice (sagittal plane), and XY-plane-slice (horizontal plane) are presented from left to right. (A1-A5) *C. corniculata* (B1-B5), *C. geniculata* (C1-C5), *T. rumicispermum* (D1-D5), *T. planicaule* (E1-E5), *T. jinghongense* (F1-F5*), C. currorii,* and *C. hastata* (G1-G5). Scale bars: (A1–G5) 1= mm.



Fig. 2. Micro-CT image used for 3D reconstruction of the seed of the representative species from the family Vitaceae. Dorsal, Ventral, YZ-plane-slice (frontal plane), XZ-plane-slice (sagittal plane), and XY-plane-slice (horizontal plane) are presented from left to right. (A1-A5) *A. brevipedunculata*, (B1-B5) *N. arborea,* (C1-C5) *A. elephantina,* (D1-D5) *V. betulifolia,* (E1-E5) *P. laetevirens,* (F1-F5) *Y. thomsonii*, (G1-G5) *L. sambucina.* Scale bars: (A1–G5) 1= mm.

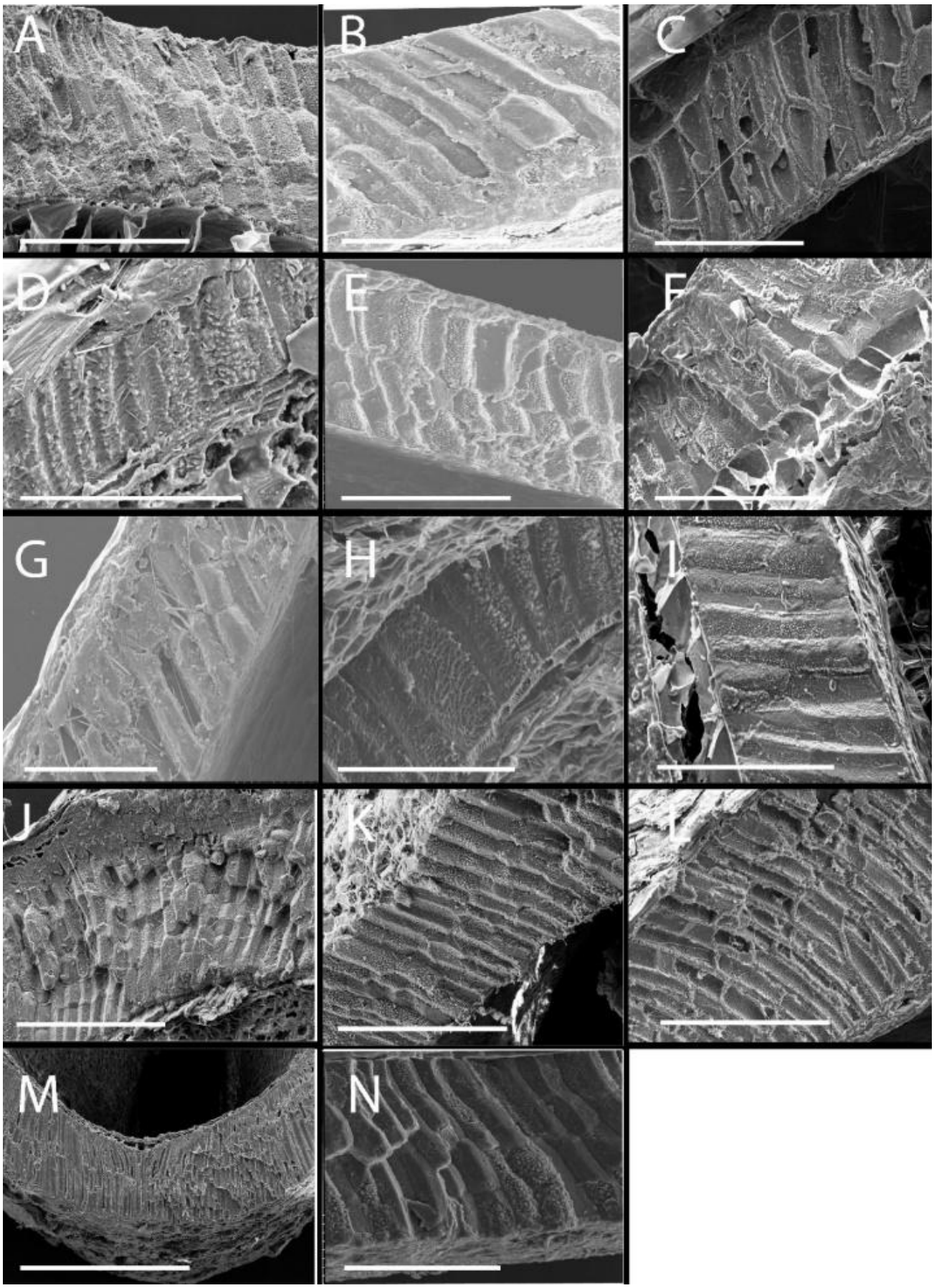


Fig. 3. The seed coat anatomy of representative species from the genus is presented using a Scanning Electron Microscope. (A) *A. elephantina*, (B) *A. brevipedunculata*, (C) *C. corniculata*, (D) *C. geniculata*, (E) *C. hastata*, (F) *C. currorii*, (G) *N. arborea*, (H) *P. laetevirens*, (I) *T. rumicispermum*, (J) *T. jinghongense*, (K) *T. planicaule*, (L) *V. betulifolia*, (M) *Y. thomsonii,* (N) *L. sambucina:* Scale bars: (A–K) =100µm, (D, G, I, L, M,) = 50µm; (N) = 40 µm.

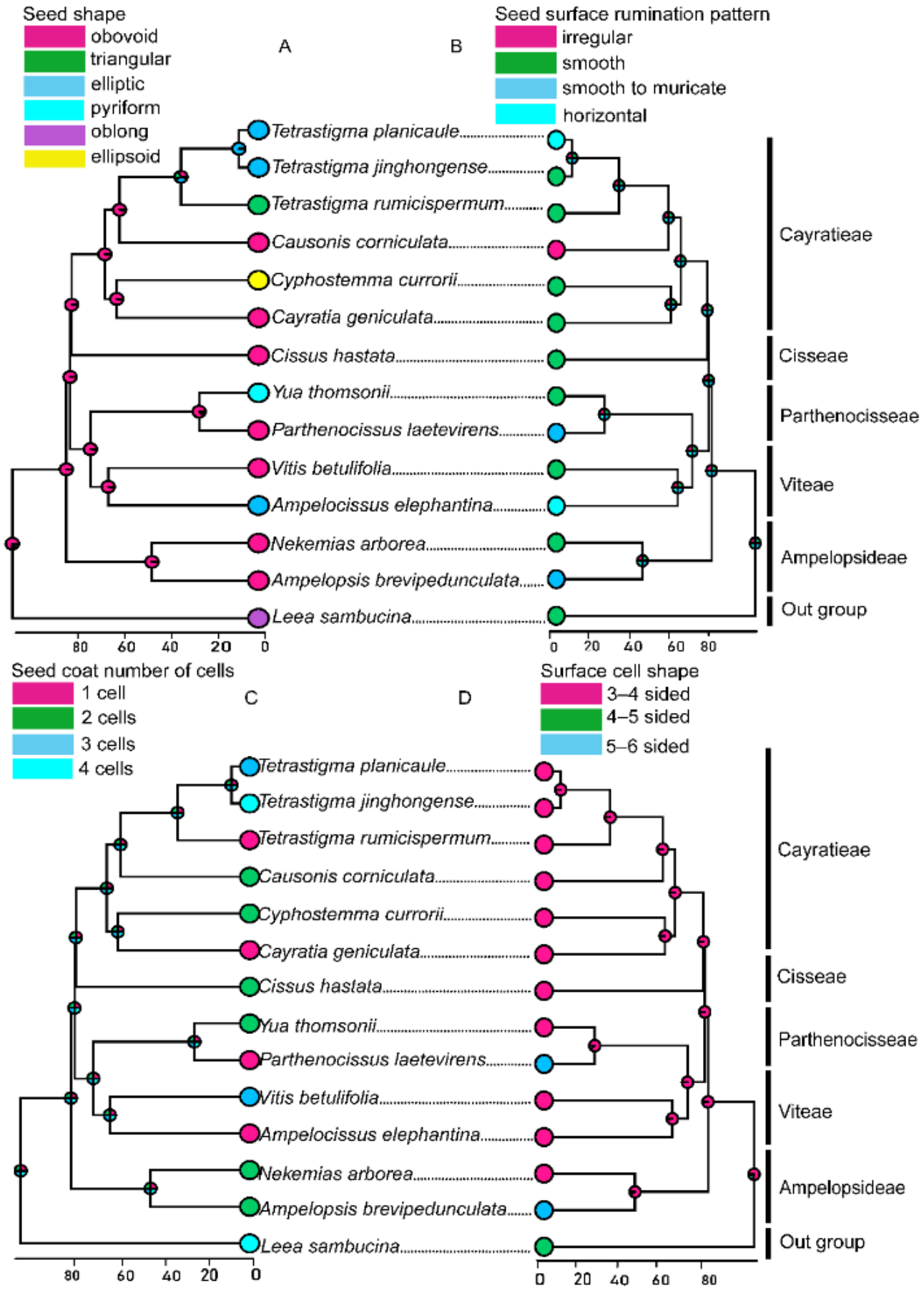


Fig. 4. Ancestral state reconstruction of seed traits on the maximum likelihood Vitaceae phylogeny. (A) Seed shape; (B) seed surface rumination pattern; (C) seed coat number of cells; (D) surface cell shape. Colors indicate observed trait states, and node pie charts show posterior probabilities of ancestral states.

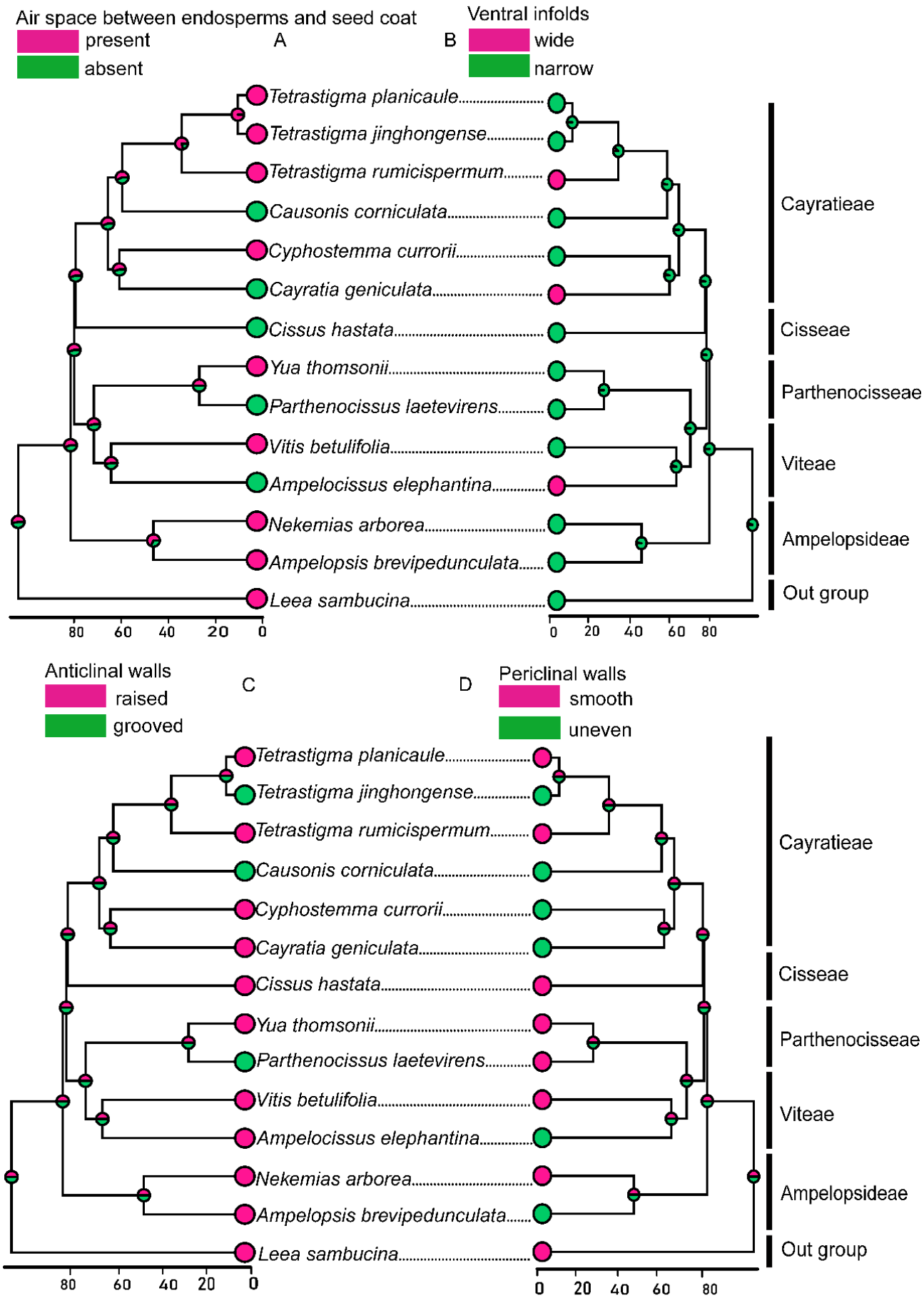


Fig. 5. Ancestral state reconstruction of the seed coat and ventral infold traits on the maximum likelihood Vitaceae phylogeny. (A) Air space between the endosperm and the seed coat; (B) ventral infolds ;(C) Anticlinal walls; (D) Periclinal walls. Colors indicate observed trait states, and node pie charts show posterior probabilities of ancestral states.

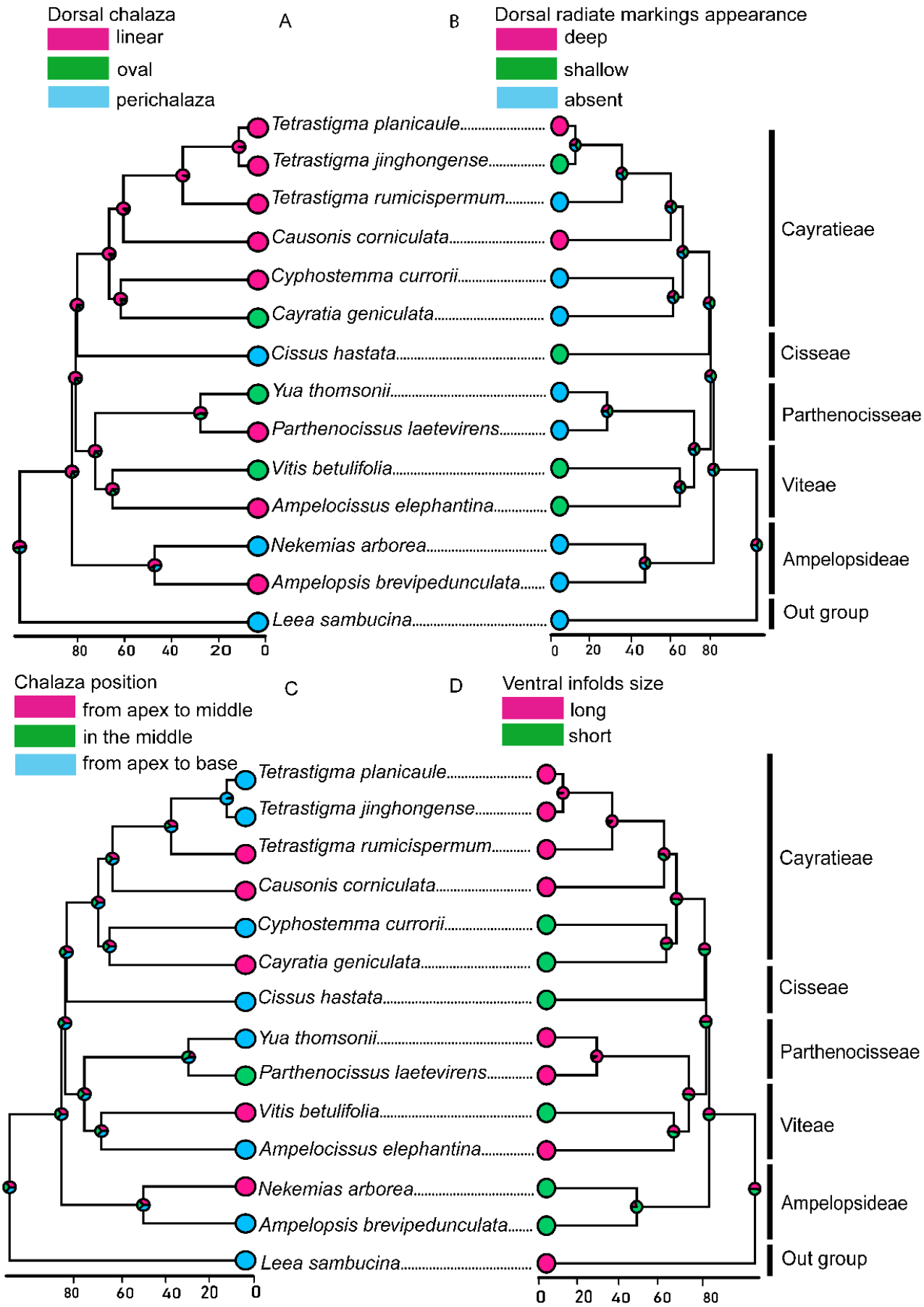


Fig. 6. Ancestral state reconstruction of dorsal chalaza, seed, and ventral infold traits on the maximum likelihood Vitaceae phylogeny. (A) Dorsal chalaza; (B) dorsal radiate markings appearance; (C) chalaza positions; (D) ventral infolds size. Colors indicate observed trait states, and node pie charts show posterior probabilities of ancestral states.

Discussion

Micro-CT was used as it allowed non-destructive high-resolution 3D visualization of both external and internal seed structures (Verboven *et al.,* 2008; Fernandes *et al.,* 2016). This method reveals features such as chalaza shape, ventral infolds, and endosperm morphology that are difficult to resolve using traditional 2D techniques (Fernandes *et al.,* 2016; Ahmed *et al.,* 2017). The present study applies micro-CT-based 3D imaging to investigate seed morphometric diversity across Vitaceae. By combining high-resolution micro-CT reconstructions with detailed morphological and anatomical observations, this study reveals substantial interspecific and intertribal variation in Vitaceae. Micro-CT allowed visualization of both external and internal features, enabling precise coding of characters related to seed shape, chalaza structure, ventral infold morphology, beak and apical notch features, transverse sectional anatomy, and quantitative dimensions of the seed and endosperm (Chen & Manchester, 2007). When these characters were mapped onto a phylogenetic framework, several traits showed associations with tribal-level patterns, while others showed extensive homoplasy. Overall, the integration of 3D anatomical data with a broad character matrix highlights the evolutionary significance of seed structure in Vitaceae and demonstrates the value of micro-CT for systematic and comparative morphological studies (Dhondt *et al.,* 2010).

Evolutionary trends of seed morphology in Vitaceae: Seed morphology has long been recognized as taxonomically and phylogenetically informative in Vitaceae (Chen and Manchester, 2007, 2011; Manchester *et al.,* 2012; Habib *et al.,* 2017, 2018). Detailed macromorphological and structural analyses have demonstrated that diagnostic characters such as chalaza architecture, ventral infolds, beak morphology, and surface ornamentation provide reliable criteria for distinguishing genera and species, as well as for identifying fossil seeds (Chen & Manchester, 2011; Manchester *et al.,* 2013). In the present study, we systematically investigated seed morphology and internal anatomy using micro-CT and SEM and reconstructed the evolution of key characters within a well-resolved phylogenetic framework. Although homoplasy is frequent across major clades, several characters provide useful morphological information for interpreting tribal-level patterns (Chen, 2009).

Seed shape in Vitaceae comprises five main forms: obovoid, triangular, ellipsoid, elliptic, and pyriform (Chen and Manchester, 2011). Ancestral reconstruction identified the obovoid form as ancestral. Seed size variation is well documented (Tcherepova & Pigg, 2005; Manchester *et al.,* 2012), with medium seed length ancestral in Cayratieae and Parthenocisseae, and short length in Cisseae and Ampelopsideae. Seed width showed tribe-specific patterns, with narrow width ancestral in Cisseae and medium width in Ampelopsideae, indicating repeated evolution of seed proportions. Surface rumination, an important taxonomic trait (Latiff, 1983; Chen & Manchester, 2011), was reconstructed as smooth in the ancestral condition and retained across most tribes. Muricate surfaces were restricted to Parthenocisseae and Ampelopsideae, suggesting lineage-specific modifications and indicating that surface sculpture is evolutionarily labile (Tiffney & Barghoorn, 1976). Beak morphology is a key feature of Vitaceae seeds (Tiffney & Barghoorn, 1976; Latiff, 2012; Habib *et al.,* 2018). Micro-CT revealed the presence of beak structures in all examined species. The prominent type was ancestral in Cisseae, Parthenocisseae, and Ampelopsideae. Beak shape shows further divergence, with conical-pointed forms ancestral in these tribes, whereas cylindrical beaks were ancestral in Cayratieae, indicating early divergence in chalazal–beak architecture (Chen & Manchester, 2011). Dorsal radiate markings vary widely across Vitaceae (Chandler, 1961; Gerrath *et al.,* 2015). The shallow type was reconstructed as ancestral for Cisseae and Viteae, whereas their absence in Parthenocisseae and Ampelopsideae indicates secondary loss. The occurrence of all states in Cayratieae suggests repeated transitions and developmental plasticity. Apical notch morphology also varies, with bilobed and retuse forms (Collinson *et al.,* 2012). The retuse type was ancestral in Cayratieae, Cisseae, and Ampelopsideae, with multiple transitions between states in other tribes, indicating that apical structures were evolutionarily dynamic and prone to homoplasy (Chen and Manchester, 2011).

Evolutionary trends of chalaza morphology in Vitaceae: Chalaza length, shape, and associated grooves are key diagnostic features of Vitaceae seeds and are widely used in taxonomy and fossil identification (Chen and Manchester, 2007, 2011). The dorsal chalaza, together with paired ventral infolds, represents a defining structural trait of the family and provides reliable criteria for distinguishing taxa (Chen & Manchester, 2007; Manchester, 2020). Our results further support the systematic value of chalaza architecture, despite repeated homoplastic transitions across tribes. A linear chalaza (length/width ratio ≥4) predominates in Cayratieae and was reconstructed as the ancestral condition for this lineage; in contrast, Cisseae shows a consistently perichalazal and elongate chalaza, indicating conserved dorsal architecture (Habib *et al.,* 2017). In contrast, Parthenocisseae, Viteae, and Ampelopsideae exhibit both linear and oval types (≤4), reflecting repeated shifts between elongate and shortened forms, consistent with previous studies (Manchester *et al.,* 2012). Chalaza length relative to seed size further differentiates lineages, with ~2/3 seed length ancestral in Cisseae and ~1/2 in Parthenocisseae (Chen & Manchester, 2007, 2011). In Cayratieae, Viteae, and Ampelopsideae, both states occur frequently, indicating multiple transitions. This suggests that chalaza proportionality is evolutionarily labile and linked to broader changes in seed architecture (Corner, 1976; Periasamy, 1962).

Chalaza length was categorized as short, medium, or long (Chen, 2009; Rajbhandary *et al.,* 2010) and showed tribe-specific trends, with a long chalaza ancestral in Cisseae and a medium chalaza in Parthenocisseae (Chen & Manchester, 2011). Chalaza width also varied, with a wide condition ancestral in Cayratieae and Parthenocisseae and a medium width in Cisseae, suggesting repeated changes in the relative dimensions of the dorsal chalazal region (Manchester *et al.,* 2012). Chalaza position provided an additional signal, with an apex-to-base position ancestral in Cisseae. In contrast, Cayratieae, Viteae, and Ampelopsideae showed both apex-to-

base and apex-to-middle states, suggesting repeated positional shifts during diversification, possibly reflecting developmental variation in the dorsal seed region (Corner, 1976). The dorsal seed surface bears a chalaza base and a groove extending toward the apex, forming an apical notch before merging with the ventral raphe (Tiffney & Barghoorn, 1976; Chen & Manchester, 2007, 2011). Ancestral reconstruction indicates a narrow and shallow chalaza–apex groove as ancestral in Parthenocisseae, whereas the groove is absent in Cisseae, highlighting clear tribal differentiation (Chen, 2009). The chalaza basal groove shows similar tribal patterns, with a narrow and shallow groove ancestral in Cayratieae and absent in Cisseae. Parthenocisseae and Viteae show no clear ancestral state, whereas Ampelopsideae exhibit both broad/deep and narrow/shallow types, indicating greater diversification (Chen, 2009). Overall, chalaza architecture, including elongation, proportions, width, position, and groove development, remains highly dynamic yet taxonomically informative in Vitaceae (Rajbhandary *et al.,* 2010). Despite frequent homoplasy, several chalazal traits show associations with tribal-level patterns consistent with molecular phylogenies, supporting their potential systematic and paleobotanical value (Tiffney & Barghoorn, 1976; Chen & Manchester, 2007, 2011; Wen *et al.,* 2007; Lu *et al.,* 2013).

Evolutionary trends of ventral infold in Vitaceae: Ventral infolds represent one of the important diagnostic characters of Vitaceae seeds and, together with the dorsal chalaza, provide reliable criteria for identifying both extant and fossil material (Chen & Manchester, 2007, 2011; Manchester *et al.,* 2012). Beyond family recognition, variation in ventral infold architecture, including length, width, size, depth, position, divergence, transverse shape, ventral view morphology, raphe structure, and external margin, has important taxonomic value and has been used to distinguish genera and interpret fossil affinities (Habib *et al.,* 2017; Popova & Yakovleva, 2009; Chen & Manchester, 2011). Ventral infold shape was categorized as narrow or wide, with the narrow type ancestral in all tribes except Viteae. Infold length showed lineage-specific trends: long in Cayratieae, medium in Ampelopsideae, and short in Cisseae (Tiffney & Barghoorn, 1976). Infold width (narrow, medium, wide) also varied, with wide ancestral in Cayratieae, narrow in Parthenocisseae and Ampelopsideae, and medium in Cisseae. Ventral infold size (short vs. long; Chen & Manchester, 2011) further supports differentiation, with the long type ancestral in Cayratieae and Parthenocisseae and the short type in Cisseae and Ampelopsideae. These patterns suggest repeated changes in infold dimensions across Vitaceae lineages (Chen, 2009). The position and divergence of ventral infolds are partly correlated. Infolds may extend along the full seed length or occupy only ½–¾ of the surface (Tiffney & Barghoorn, 1976; Chen, 2009). A full-length infold was ancestral in Parthenocisseae, whereas Cisseae and Ampelopsideae had shorter infolds (½–¾ seed length) (Chen, 2009). Divergence from the seed base was ancestral in Cayratieae, Cisseae, and Parthenocisseae, with an independent middle divergence within Cayratieae. Micro-CT revealed further variation in ventral infold morphology. The keel-shaped type was ancestral in Cayratieae, Cisseae, Parthenocisseae, and Ampelopsideae (Chen & Manchester, 2007, 2011), whereas in Viteae, obelliptic and furrowed forms evolved independently, indicating increased structural diversification (Popova & Yakovleva, 2009).

The raphe, forming a ridge between paired infolds, shows phylogenetic structure, with almost aequilate and tapering forms (Xiang *et al.,* 2021). The almost aequilate type was ancestral in Cayratieae and Cisseae, whereas the tapering form was ancestral in Viteae. Ventral holes, expressed as paired furrows (Popova & Yakovleva, 2009; Latiff, 2012), were ancestrally reconstructed as base-to-apex furrows in most tribes, except Cisseae, where a middle-to-apex furrow was ancestral. External margins of ventral infolds were predominantly smooth, with rough margins representing derived states, especially in Viteae (Manchester *et al.,* 2012). In transverse view, concave infolds were ancestral in Cayratieae, Cisseae, Parthenocisseae, and Ampelopsideae, while in Viteae, both concave and horseshoe forms evolved independently, indicating greater diversification (Chen, 2009). Infold depth provides additional morphological variation among lineages, with ¾ seed-length depth ancestral in most tribes and shallower (½) infolds in Cisseae (Cervantes *et al.,* 2021).

Evolutionary trends of endosperm and seed coat anatomy in Vitaceae: Vitaceae seeds are characterized by an endotestal seed coat and a typically ruminate endosperm, with rumination arising from integumentary ingrowths in the ventral (raphe) region (Periasamy, 1962; Corner, 1976; Chen & Manchester, 2007). These features are diagnostic for the family and important in both extant and fossil systematics (Manchester *et al.,* 2013). Our results reveal a combination of ancestral patterns and repeated lineage-specific modifications in endosperm organization and seed coat structure. Endosperm shape varies markedly across Vitaceae (Chen, 2009). An M-shaped endosperm was ancestral in Cisseae and Viteae, whereas Cayratieae shows greater diversity (M-, m-, U-shaped, and modified forms), indicating diversification of endosperm configurations (Abid *et al.,* 2014). Endosperm length (short, medium, long; Periasamy, 1962) also shows tribal differentiation, with long endosperm ancestral in Cayratieae and Cisseae and short in Viteae. Endosperm width further supports this pattern, with medium width ancestral in Cayratieae and narrow width in Cisseae, suggesting changes in internal packing rather than simple scaling (Corner, 1976; Chen, 2009). Micro-CT revealed variation in transverse-section dimensions: Cayratieae and Cisseae typically exhibit greater height, indicating an elongated internal structure, whereas Viteae and Ampelopsideae show reduced or intermediate heights (Periasamy, 1962; Manchester *et al.,* 2020). Width patterns are similar, with a wide condition ancestral in Cayratieae and medium in Cisseae and Ampelopsideae, indicating independent evolution of internal seed geometry (Corner, 1976). The vitaceous testa, derived from the outer integument, comprises a soft sarcotesta and a lignified endotesta (Corner, 1976). Endotesta thickness varies widely and may contribute to differences in seed coat structure and protection (Manchester *et al.,* 2013). Overall thickness was ancestral as thick in Cayratieae and Cisseae, whereas Parthenocisseae, Viteae, and Ampelopsideae show all states, indicating repeated gains and reductions

(Corner, 1976). Regional patterns further highlight this variation: at the chalaza, medium thickness was ancestral in Cisseae and Parthenocisseae, with independent shifts in Cayratieae; at the ruga sinus, medium thickness was ancestral in Cayratieae, while thick endotesta characterized Cisseae and Viteae (Manchester *et al.,* 2013, 2020). These patterns suggest region-specific contributions to seed coat diversification (Chen & Manchester, 2007).

Seed coat cellular structure is known to vary substantially in Vitaceae (Periasamy, 1962; Manchester *et al.,* 2013). Differences in sclereid layering have been used to distinguish genera, including reports of single-layer endotesta in *Parthenocissus* and more complex biseriate or multilayered conditions in other taxa (Chen, 2009). A two-layer seed coat was reconstructed as ancestral in Cayratieae and Ampelopsideae (Cervantes *et al.,* 2021). A single-layer condition occurred independently in Cayratieae, Parthenocisseae, and Viteae, suggesting convergent reduction of seed coat complexity (Manchester, 2020). In contrast, three- and four-layer conditions evolved within Cayratieae, with the four-layer state representing the greatest structural elaboration. Surface cell morphology further reflects evolutionary divergence (Lu *et al.,* 2012; Manchester *et al.,* 2013). A 3–4-sided epidermal cell shape was ancestral in Cayratieae and Viteae, whereas 5–6-sided shapes evolved independently in Parthenocisseae and Ampelopsideae, supporting earlier reports of taxonomic significance in seed coat micromorphology (Latiff, 1983; Manchester *et al.,* 2020). The presence of air space between endosperm and seed coat was ancestral in Cayratieae and Ampelopsideae but absent in Cisseae, with multiple independent gains and losses across tribes. The anticlinal wall structure exhibited two states: raised and grooved (Lu *et al.,* 2012; Cervantes *et al.,* 2021). Raised walls were ancestral in most tribes, whereas grooved walls evolved convergently. Wall thickness also displayed phylogenetic structure, with thick walls ancestral in Cayratieae, Parthenocisseae, and Viteae, and thin walls ancestral in Cisseae (Lu *et al.,* 2012). Periclinal wall structure (smooth vs. uneven) further highlights evolutionary lability, with uneven walls ancestral in Cayratieae and smooth walls in Cisseae and Parthenocisseae. These patterns highlight the diversity and evolutionary variation of testa microstructure across the family (Manchester *et al.,* 2013).

Ecological significance of seed coat ornamentation in Vitaceae: Seed coat ornamentation in Vitaceae is highly diverse and taxonomically informative (Chen & Manchester, 2007; Xiang *et al.,* 2021), although its ecological significance remains less explored. Vitaceous seeds possess an endotestal seed coat and a ruminate endosperm formed by integumentary ingrowths in the ventral (raphe) region (Periasamy, 1962; Tiffney & Barghoorn, 1976). Variation in these ingrowths reflects differences in perichalazal development and is both phylogenetically informative and evolutionarily labile (Manchester *et al.,* 2013; Habib *et al.,* 2017). Micro-CT and SEM analyses show that internal seed traits, endosperm shape, endotesta structure, air space, and seed coat layering are closely linked to surface ornamentation and epidermal wall architecture (Periasamy, 1962), indicating coordinated evolution of internal and external features. Such integration may reflect adaptive responses to ecological pressures (Abid *et al.,* 2016). Dispersal likely influences these traits, as many Vitaceae species are animal-dispersed, including by monkeys (Agmen *et al.,* 2010), civets and macaques (Cervantes *et al.,* 2021), and birds (Lok *et al.,* 2011), while some *Leea* species may disperse via ocean drift (Latiff, 1983). Seed coat ornamentation (e.g., ruminations, ridges, muricate surfaces) may enhance protection during gut passage, resist abrasion, and improve soil retention and anchorage (Lombardi, 2007; 2015). Seed coat complexity may influence water uptake and germination. Variations in seed morphology affect hydration patterns (Berry, 1927), while endotesta thickness (Chen & Manchester, 2007), sclereid layering (Periasamy, 1962), and anticlinal/periclinal wall structure (Lu *et al.,* 2012) likely regulate permeability and resistance to desiccation. Internal features such as ruminate endosperm and air spaces may further influence hydration dynamics and embryo expansion under contrasting environments (Chen & Manchester, 2007; Manchester *et al.,* 2020). Overall, increased seed coat ornamentation and structural complexity in Vitaceae reflect lineage-specific ecological modifications built upon a conserved ancestral architecture, shaped by both phylogeny and environment (Manchester *et al.,* 2013). Although functional interpretations remain largely inferential, integrating 3D internal anatomy with surface micromorphology highlights the ecological relevance of seed traits and the value of micro-CT (Chen, 2009; Latiff, 2012). Future studies combining germination experiments, biomechanics, and ecological data will be essential to clarify how seed morphology influences dispersal, dormancy, and establishment (Berry, 1927; Fernandes *et al.,* 2016; Ahmed *et al.,* 2017).

Conclusion

This study demonstrates that micro-computed tomography (micro-CT), combined with detailed morphometric analyses, provides a powerful and non-destructive approach for revealing three-dimensional seed morphology and internal anatomy in Vitaceae. Across all the studied species, seeds showed pronounced variation in size, shape, chalaza architecture, ventral infolds, endosperm configuration, and seed coat structure. Many of these characters, particularly chalaza-related traits, ventral infold morphology, endotesta thickness, and endosperm shape, show clear patterns of variation and contribute to distinguishing genera and tribes. The integration of quantitative morphometrics, PCA, correlation analyses, and ancestral state reconstruction highlights the evolutionary significance of internal seed traits that are often inaccessible through traditional methods. Overall, these results establish micro-CT–based seed morphology as a robust framework for comparative systematics, evolutionary inference, and trait-based classification within Vitaceae.

Funding: This study was supported by the Key Special Project of the National Key R&D Plan "Research on Key Technologies of Biosafety" (2022YFC2601200). Research on Safety Risk Assessment and Early Warning System of Important Strategic Biological Resources (Nov 2022-Oct 2025). S.U. was supported by the Chinese Government Scholarship for International PhD Students.

Acknowledgements

The authors sincerely thank Xiu-Ping Xu for her guidance and technical support with the Scanning Electron Microscopy (SEM) and micro-CT analyses. We are grateful to the Institute of Botany, Chinese Academy of Sciences, for providing the research facilities. Their technical expertise and institutional support significantly contributed to this study.

Author's Contributions: B.L., L.-M.L. and Z.-D.C. designed the study. S.U. and K.N. performed the research and analyzed the data. L.-M.L. and R.N.R. conceived the methodology. S.U. and K.N. conducted the investigation. S.U., K.N., L.-M.L. and R.N.R. wrote the original draft. Z.-D.C., Z.-Y.T., B.L., S.A., M.A., C.-C.Z., and L.-N.Z. reviewed and edited the manuscript. Z.-D.C. and L.-M.L. acquired funding. All authors read and approved the manuscript.

Conflicts of Interest: The authors declare no conflicts of interest.

Data Availability: The supplementary data supporting this study, including supplementary figures and tables, are available in the Science Data Bank repository under the dataset title Three-Dimensional Seed Morphology and Evolutionary Diversification in the Grape Family (Vitaceae) (Version 1). The dataset can be accessed at https://doi.org/10.57760/sciencedb.018zl.

References

Abid, R., A. Ather and M. Qaiser. 2016. Seed morphology and its taxonomic significance in the family Malvaceae. *Pak. J. Bot.*, 48(6): 2307-2341.

Abid, R., D. Kanwal and M. Qaiser. 2014. Seed morphological studies on some monocot families (excluding Gramineae) and their phylogenetic implications. *Pak. J. Bot.*, 46(4): 1309-1324.

Adams, N.F., M.E. Collinson, S.Y. Smith, M.K. Bamford, F. Forest, P. Malakasi, F. Marone and D. Sykes. 2016. X-rays and virtual taphonomy resolve the first *Cissus* (Vitaceae) macrofossils from Africa as early-diverging members of the genus. *Am. J. Bot.*, 103(9): 1657–1677. https://doi.org/10.3732/ajb.1600177

Agmen, F.L., H.M. Chapman and M. Bawuro. 2010. Seed dispersal by tantalus monkeys (*Chlorocebus tantalus tantalus*) in a Nigerian montane forest. *Afr. J. Ecol.*, 48: 1123-1128. https://doi.org/10.1111/j.1365-2028.2009.01190.x

Ahmed, M.R., J. Yasmin and W.H. Lee. 2017. Imaging technologies for nondestructive measurement of internal properties of agricultural products: A review. *J. Biosyst. Eng.*, 42(3): 199-216. https://doi.org/10.5307/JBE.2017.42.3.199

Anonymous. 2025. *Plants of the World Online.* Facilitated by the Royal Botanic Gardens, Kew. Published on the Internet; http://www.plantsoftheworldonline.org/.Retrieved 23 April 2026.

Berry, E.W. 1927. Seed remains from the Eocene of North America. *Bull. Torrey Bot. Club*, 54: 195-209.

Blomberg, S.P., T. Garland and A.R. Ives. 2003. Testing for phylogenetic signal in comparative data. *Evolution*, 57(4): 717-745. https://doi.org/10.1111/j.0014-3820.2003.tb00285.x

Budha-Magar, S., P. Bhandari and S.K. Ghimire. 2020. Ethno-medicinal survey of plants used by Magar (Kham) community, Rolpa district, Western Nepal. *Ethnobot. Res. Appl.*, 19: 1-29. https://doi.org/10.32859/era.19.18.1-29

Cazaux, J. 2005. Recent developments and new strategies in scanning electron microscopy. *J. Microsc.*, 217(1): 16-35. https://doi.org/10.1111/j.0022-2720.2005.01414.x

Cervantes, E., J.J. Martín-Gómez, D. Gutiérrez del Pozo and Á. Tocino. 2021. Seed geometry in the Vitaceae. *Plants*, 10(8): 1695. https://doi.org/10.3390/plants10081695

Chandler, M.E.J. 1961. The Lower Tertiary Floras of Southern England. London: *British Museum.*

Chen, I. 2009. History of Vitaceae inferred from morphology-based phylogeny and the fossil record of seeds. PhD Thesis, *University of Florida, Gainesville, USA.*

Chen, I. and S.R. Manchester. 2007. Seed morphology of modern and fossil *Ampelocissus* (Vitaceae) and implications for phytogeography. *Am. J. Bot.*, 94(9): 1534-1553. https://doi.org/10.3732/ajb.94.9.1534

Chen, I. and S.R. Manchester. 2011. Seed morphology of Vitaceae. *Int. J. Plant Sci.*, 172(1): 1-35. https://doi.org/10.1086/657283

Cho, S.H., J.H. Lee, D.H. Kang and B.Y. Kim. 2016. *Cissus erecta* (Vitaceae), a new non-viny herbaceous species from Mt. Popa, Myanmar. *Phytotaxa*, 260(3): 291-295. https://doi.org/10.11646/phytotaxa.260.3.9

Collinson, M.E., S.R. Manchester and V. Wilde. 2012. Fossil seeds and fruits of Vitaceae. *Rev. Palaeobot. Palynol.*, 170: 1-28.

Corner, E.J.H. 1976. *The Seeds of Dicotyledons*. Cambridge: Cambridge University Press.

Dang, V.C., L.M. Lu and V.H. Nguyen. 2016. A new record of the genus *Yua* (Vitaceae) from Vietnam. *Phytotaxa*, 255(3): 274-280. https://doi.org/10.11646/phytotaxa.255.3.9

Dang, V.C., V.H. Nguyen, B. Dao, W. Yang, F. Li, X. Yang and L.M. Lu. 2017. A new species and new records of *Cyphostemma* (Vitaceae) from China and Vietnam based on morphological and molecular evidence. *Syst. Bot.*, 42(3): 449-457. https://doi.org/10.1600/036364417X696032

Dhondt, S., H. Vanhaeren, D. Van Loo, V. Cnudde and D. Inzé. 2010. Plant structure visualization by high-resolution X-ray computed tomography. *Trends Plant Sci.*, 15(8): 419-422. https://doi.org/10.1016/j.tplants.2010.05.002

Diels, E., M. van Dael, J. Keresztes, S. Vanmaercke, P. Verboven, B. Nicolai and B. Smeets. 2017. Assessment of bruise volumes in apples using X-ray computed tomography. *Postharvest Biol. Technol.*, 128: 24-32. https://doi.org/10.1016/j.postharvbio.2017.01.013

Dorofeev, P.I. 1957. Seeds of *Ampelopsis* from the Tertiary deposits of the territory of USSR. *Bot. Zhurn. (Moscow & Leningrad)*, 42: 643-648.

Fernandes, A.M., P. Verboven and E. Herremans. 2016. Image processing for food microstructure analysis. *Food Control*, 59: 1-10.

Gerrath, J., U. Posluszny and L. Melville. 2015. *Taming the Wild Grape: Botany and Horticulture in the Vitaceae*. Springer, New York, USA. https://doi.org/10.1007/978-3-319-24352-8

Gerrath, J.M. and U. Posluszny. 1989. Morphological and anatomical development in the Vitaceae. III. Vegetative development in *Parthenocissus inserta*. *Can. J. Bot.*, 67(3): 803-816.

Gerrath, J.M., U. Posluszny, S.M. Ickert-Bond and J. Wen. 2017. Inflorescence morphology and development in the basal rosid lineage Vitales. *J. Syst. Evol.*, 55(6): 542-558. https://doi.org/10.1111/jse.12261

Godfray, H.C.J. and S. Knapp. 2004. Taxonomy for the twenty-first century. *Phil. Trans. R. Soc. B*, 359(1444): 559-569. https://doi.org/10.1098/rstb.2003.1457

Habib, S., V.C. Dang, S.M. Ickert-Bond, J. Wen, Z.D. Chen and L.M. Lu. 2018. Evolutionary trends in *Tetrastigma* (Vitaceae): Morphological diversity and taxonomic implications. *J. Syst. Evol.*, 56(4): 360-373. https://doi.org/ 10.1111/jse.12222

Habib, S., V.C. Dang, S.M. Ickert-Bond, J.L. Zhang, L.M. Lu, J. Wen and Z.D. Chen. 2017. Robust phylogeny of *Tetrastigma* (Vitaceae) based on ten plastid DNA regions: Implications for infrageneric classification and seed character evolution. *Front. Plant Sci.*, 8: 590. https://doi.org/10.3389/fpls. 2017.00590

Heywood, V.H. 1969. Scanning electron microscopy in the study of plant materials. *Micron*, 1(1): 1-14. https://doi.org/10.1016/0047-7206(69)90002-8

Jackes, B.R. and A. Trias-Blasi. 2023. *Apocissus* Jackes & Trias-Blasi, a new genus in the Vitaceae. *Austrobaileya*, 13: 94-104. https://doi.org/10.5962/p.411120

Karkamkar, S.P., S.G. Patil and S.C. Misra. 2010. Cyto-morphological studies and their significance in evolution of family Vitaceae. *Nucleus*, 53(1-2): 37-43. https://doi.org/10.1007/s13237-010-0009-6

Latiff, A. 1982. Studies in Malesian Vitaceae. *Fed. Mus. J.*, 27: 42-74.

Latiff, A. 1983. The genus *Tetrastigma* in the Malay Peninsula. *Gard. Bull. Singapore*, 36: 213-228.

Latiff, A. 2012. Seed morphology of *Parthenocissus* Planch. and *Ampelopsis* Michx. (Vitaceae) and its taxonomic significance. *Sains Malaysiana*, 41(12): 1503-1508.

Liu, X.Q., S.M. Ickert-Bond, L.Q. Chen and J. Wen. 2013. Molecular phylogeny of *Cissus* L. of Vitaceae (the grape family) and evolution of its pantropical intercontinental disjunctions. *Mol. Phylogenet. Evol.*, 66(1): 43-53. https://doi.org/10.1016/j.ympev.2012.09.003

Liu, X.Q., S.M. Ickert-Bond, Z.L. Nie and J. Wen. 2016. Phylogeny of the *Ampelocissus–Vitis* clade in Vitaceae supports the New World origin of the grape genus. *Mol. Phylogenet. Evol.*, 95: 217-228. https://doi.org/10.1016/j.ympev.2015.10.013

Lok, A.F.S.L., W.F. Ang, B.Y.Q. Ng, S.M. Suen, C.K. Yeo and H.T.W. Tan. 2011. Leea L. (Vitaceae) of Singapore. Nat. Singapore, 4: 55-71.

Lombardi, J.A. 2007. Systematics of Vitaceae in South America. *Can. J. Bot.*, 85(8): 712-721. https://doi.org/10.1139/B07-021

Lombardi, J.A. 2015. New combinations for the South American *Cissus striata* clade (Vitaceae). *Phytotaxa*, 227(3): 295-298. https://doi.org/10.11646/phytotaxa.227.3.10

Lu, L., J. Wen and Z.D. Chen. 2016. *Cayratia cheniana* (Vitaceae): An endangered new species endemic to the limestone mountains of Ninh Thuan Province, Vietnam. *Syst. Bot.*, 41(1): 49-55. https://doi.org/10.1600/036364416X690741

Lu, L.M., C.J. Cox, S. Mathews, W. Wang, J. Wen and Z.D. Chen. 2018a. Optimal data partitioning, multispecies coalescent and Bayesian concordance analyses resolve early divergences of the grape family (Vitaceae). *Cladistics*, 34(1): 57-77. https://doi.org/10.1111/cla.12191

Lu, L.M., J. Wen and Z.D. Chen. 2012. A combined morphological and molecular phylogenetic analysis of *Parthenocissus* (Vitaceae) and taxonomic implications. *Bot. J. Linn. Soc.*, 168(1): 43-63. https://doi.org/10.1111/j.1095-8339.2011.01186.x

Lu, L.M., S.M. Ickert-Bond and J. Wen. 2018b. Recent advances in systematics and evolution of the grape family Vitaceae. *J. Syst. Evol.*, 56(4): 259-261. https://doi.org/10.1111/jse.12449

Lu, L.M., W. Wang, Z.D. Chen and J. Wen. 2013. Phylogeny of the non-monophyletic *Cayratia* Juss. (Vitaceae) and implications for character evolution and biogeography. *Mol. Phylogenet. Evol.*, 68(3): 502-515. https://doi.org/10.1016/j.ympev.2013.04.023

Lubna, M.Z. Zafar and M. Ahmad. 2021. SEM-based palynological characterization of Vitaceae. *Microsc. Res. Tech.*, 84: 608-617. https://doi.org/10.1002/jemt.23619

Ma, Z.Y., Z.L. Nie, C. Ren, X.Q. Liu, E.A. Zimmer and J. Wen. 2021. Phylogenomic relationships and character evolution of the grape family (Vitaceae). *Mol. Phylogenet. Evol.*, 154: 106948. https://doi.org/10.1016/j.ympev.2020.106948

Manchester, S.R. 1994. *Fruits and seeds of the Middle Eocene Nut Beds Flora, Clarno Formation, Oregon*. *Palaeontogr. Am.*, 58: 1-205.

Manchester, S.R. 2020. Morphology and affinities of *Ampelocissites* seeds (Vitaceae: Ampelopsis clade) from the Paleogene of Texas, USA. *Syst. Bot.*, 45(3): 478-482. https://doi.org/10.1600/036364420X15935294613400

Manchester, S.R., D.K. Kapgate and J. Wen. 2013. Oldest fruits of the grape family (Vitaceae) from the Late Cretaceous Deccan cherts of India. *Am. J. Bot.*, 100(9): 1849-1859. https://doi.org/10.3732/ajb.1300008

Manchester, S.R., I. Chen and T.A. Lott. 2012. Seeds of *Ampelocissus*, *Cissus*, and *Leea* (Vitaceae) from the Paleogene of western Peru and their biogeographic significance. *Int. J. Plant Sci.*, 173(8): 933-943. https://doi.org/10.1086/667233

Moreau, J.D., P. Cloetens, B.D. Gomez, V. Daviero-Gomez, A. Nel, P. Tafforeau and V. Perrichot. 2014. Multiscale 3D virtual dissections of 100-million-year-old flowers using X-ray synchrotron micro-nano tomography. *Microsc. Microanal.*, 20(1): 305-312.

Myles, S., A.R. Boyko, C.L. Owens, P.J. Brown, F. Grassi, M.K. Aradhya, B. Prins, A. Reynolds, J.M. Chia, D. Ware, C.D. Bustamante and E.S. Buckler. 2011. Genetic structure and domestication history of the grape. *Proc. Natl. Acad. Sci. USA*, 108(9): 3530-3535. https://doi.org/10.1073/pnas.1009363108

Najmaddin, C., K. Hussin and H. Maideen. 2013. Comparative leaf anatomy of selected species in *Vitaceae* and *Leeaceae*. *Am. J. Appl. Sci.*, 10(4): 414-417. https://doi.org/10.3844/ajassp.2013.414.417

Nie, Z.L., H. Sun, S.R. Manchester, Y. Meng, Q. Luke and J. Wen. 2012. Evolution of the intercontinental disjunctions in six continents in the *Ampelopsis* clade of the grape family (Vitaceae). *BMC Evol. Biol.*, 12: 17. https://doi.org/10.1186/1471-2148-12-17

Nie, Z.L., H. Sun, Z.D. Chen, Y. Meng, S.R. Manchester and J. Wen. 2010. Molecular phylogeny and biogeographic diversification of *Parthenocissus* (Vitaceae) disjunct between Asia and North America. *Am. J. Bot.*, 97(8): 1342-1353. https://doi.org/10.3732/ajb.1000085

Pagel, M. 1999. Inferring the historical patterns of biological evolution. Nature, 401: 877-884. https://doi.org/10.1038/44766

Parmar, G., V.C. Dang, R.N. Rabarijaona, Z.D. Chen, B.R. Jackes, R.L. Barrett, J. Wen and L.M. Lu. 2021. Phylogeny, character evolution and taxonomic revision of *Causonis*, a segregate genus from *Cayratia* (Vitaceae). *Taxon*, 70: 1188-1218. https://doi.org/10.1002/tax.12562

Periasamy, K. 1962. Studies on seeds with ruminate endosperm. II. Development of rumination in the Vitaceae. *Proc. Indian Acad. Sci. B*, 56(1): 13-26.

Popova, S.S. and O.V. Yakovleva. 2009. Seed morphology and anatomy of extant and fossil species of *Vitis* and *Ampelopsis* (Vitaceae). *Bot. Zhurn.*, 94(11): 1647-1657.

Rabarijaona, R.N., J.R. Yu, Z.Y. Tang, R.M. Ranaivoson, R.L. Barrett, M. Rakotoarinivo, B. Liu, Y.C. You, S.S. Yaradua, G. Romeo, J. Wen, Z.D. Chen and L.M. Lu. 2025. Phylogenomic insights into historical biogeography and species delimitation of African *Ampelocissus* (Vitaceae). *Mol. Phylogenet. Evol.*, 211: 108388. https://doi.org/10.1016/j.ympev.2025.108388

Rabarijaona, R.N., V.C. Dang, G. Parmar, B. Liu, J. Wen, Z.D. Chen and L.M. Lu. 2020. Phylogeny and taxonomy of *Afrocayratia*, a new genus of Vitaceae from continental Africa and Madagascar. *J. Syst. Evol.*, 58(6): 1090-1107. https://doi.org/10.1111/jse.12697

Rabarijaona, R.N., V.L. Rafaralahy, C. Rakotovao, R.M. Ranaivoson, B. Liu, Z.D. Chen, J. Wen and L.M. Lu. 2021. *Cyphostemma calcarium*, a new species of Vitaceae from the Ankarana Special Reserve, Madagascar. *PhytoKeys*, 180: 73-80. https://doi.org/10.3897/phytokeys.180.69194

Rajbhandary, S. and K.K. Shrestha. 2010. Taxonomic and ecological significance of seed micromorphology in Himalayan *Begonias*: SEM analysis. *Pak. J. Bot.*, 42: 135-154.

Revell, L.J. 2012. phytools: an R package for phylogenetic comparative biology (and other things). *Methods Ecol. Evol.*, 3(2): 217-223. https://doi.org/10.1111/j.2041-210X.2011.00169.x

Rossetto, M., D.M. Crayn, B.R. Jackes and C. Porter. 2007. An updated estimate of intergeneric phylogenetic relationships in the Australian Vitaceae. *Can. J. Bot.*, 85(8): 722-730. https://doi.org/10.1139/B07-022

Rozefelds, A.C. and M.R. Pace. 2018. The first record of fossil Vitaceae wood from the Southern Hemisphere, a new combination for *Vitaceoxylon ramunculiformis*, and reappraisal of the fossil record of the grape family (Vitaceae) from the Cenozoic of Australia. *J. Syst. Evol.*, 56(4): 283-296. https://doi.org/10.1111/jse.12300

Schmid, R. 1986. Terminology of angiosperm seed coats. Taxon, 35: 476-491.

Soejima, A. and J. Wen. 2006. Phylogenetic analysis of the grape family (*Vitaceae*) based on three chloroplast markers. *Am. J. Bot.*, 93(2): 278-287. https://doi.org/10.3732/ajb.93.2.278

Soltis, D.E., P.S. Soltis and M.W. Chase. 2000. Angiosperm phylogeny inferred from 18S rDNA, *rbcL*, and *atpB* sequences. *Bot. J. Linn. Soc.*, 133(4): 381-461. https://doi.org/10.1093/botlinnean/133.4.381

Song, Y.X., S. Peng, F.M. Mutie, H. Jiang, J. Ren, Y.Y. Cong and G.W. Hu. 2022. Evolution and taxonomic significance of seed micromorphology in *Impatiens* (Balsaminaceae). *Front. Plant Sci.*, 13: 835943. https://doi.org/10.3389/fpls.2022.835943

Sun, C., E. Müller, M. Meffert and D. Gerthsen. 2018. On the progress of scanning transmission electron microscopy (STEM) imaging in a scanning electron microscope. *Microsc. Microanal.*, 24(2): 99-106. https://doi.org/10.1017/S1431927618000181

Süssenguth, K. 1953. Vitaceae. In: (Eds.): Engler, A. and K. Prantl. *Die Natürlichen Pflanzenfamilien*. Berlin: Duncker & Humblot, 20(8): 174-333.

Tiffney, B.H. and E.S. Barghoorn. 1976. Fruits and seeds of the Brandon Lignite. I. Vitaceae. *Rev. Palaeobot. Palynol.*, 22: 169-191. https://doi.org/10.1016/0034-6667(76)90001-4

Timmons, S.A., U. Posluszny and J.M. Gerrath. 2007. Morphological and anatomical development in the Vitaceae. IX. Comparative ontogeny and phylogenetic implications of *Vitis rotundifolia* Michx. *Botany*, 85(9): 850-859. https://doi.org/10.1139/B07-077

Trias-Blasi, A., M. Poopath, L.M. Lu and G. Parmar. 2021. *Causonis sessilifolia* (Vitaceae), a new species from Thailand. *PhytoKeys*, 185: 55-64. https://doi.org/10.3897/phytokeys.185.75570

Verboven, P., E. Herremans, T. Defraeye, S. Rogge, Q.T. Ho, M.L. Hertog, B.E. Verlinden, E. Bongaers, M. Wevers and B.M. Nicolai. 2014. X-ray CT for quantitative food microstructure engineering: The apple case. *Nucl. Instrum. Methods Phys. Res. B*, 324: 88-94. https://doi.org/10.1016/j.nimb.2013.07.035

Wen, J. 2007. Leeaceae. In: Kubitzki, K. (Ed.), *The Families and Genera of Vascular Plants*. Vol. 9. Flowering Plants. Eudicots. Berlin: Springer, pp. 221-225. https://doi.org/10.1007/978-3-540-32219-1_29

Wen, J., A.J. Harris, Y. Kalburgi, N. Zhang, Y. Xu, W. Zheng, S.M. Ickert-Bond, G. Johnson and E.A. Zimmer. 2018. Chloroplast phylogenomics of the New World grape species (Vitis, Vitaceae). *J. Syst. Evol*., 56(4): 297-308. https://doi.org/10.1111/jse.12325.

Wen, J., J.K. Boggan and Z.L. Nie. 2014. Synopsis of *Nekemias* Raf., a segregate genus from *Ampelopsis* Michx. (Vitaceae) disjunct between eastern/southeastern Asia and eastern North America, with ten new combinations. *PhytoKeys*, 42: 11-19. https://doi.org/10.3897/phytokeys.42.7704

Wen, J., L.M. Lu and J.K. Boggan. 2013. Diversity and evolution of Vitaceae in the Philippines. *Philipp. J. Sci.*, 142(Special Issue): 223-244.

Wilson, T., J.M. Gerrath and U. Posluszny. 2006. Morphological and anatomical development in the Vitaceae. VIII. Comparative development of three Cyphostemma (Vitaceae) species reveals important vegetative and reproductive differences among the species. *Can. J. Bot*., 84(5): 702-716. https://doi.org/10.1139/b06-022

Xiao, Y., J. Wen, R. Meng, Y. Meng, Q. Zhou and Z.L. Nie. 2021. The expansion and diversity of the CYP75 gene family in Vitaceae. *Peer J*., 9: e12174. https://doi.org/10.7717/peerj.12174

You, Y., J. Yu, Z. Nie, D. Peng, R.L. Barrett, R.N. Rabarijaona, Y. Lai, Y. Zhao, V.C. Dang, Y. Chen, Z.D. Chen and J. Wen. 2024. Transition of survival strategies under global climate shifts in the grape family. *Nat. Plants*, 10(7): 1100-1111. https://doi.org/10.1038/s41477-024-01726-8